DEVELOPMENT OF A NOVEL METHOD FOR MEASURING THE TRANSVERSE PIEZOELECTRIC COEFFICIENTS OF THIN PIEZOELECTRIC FILMS

By

TIMOTHY MICHAEL SULLIVAN

A thesis submitted in partial fulfillment of
the requirements for the degree of

MASTER OF SCIENCE IN MATERIALS SCIENCE AND ENGINEERING

WASHINGTON STATE UNIVERSITY
School of Mechanical and Materials Engineering

AUGUST 2004

To the Faculty of Washington State University:

The members of the committee appointed to examine the thesis of TIMOTHY MICHAEL SULLIVAN find it satisfactory and recommend that it be accepted.

_____
Chair

_____

_____

ACKNOWLEDGMENT

I would like to thank my family and friends for their encouragement and support during the entirety of my education. I owe special appreciation to Amanda who endured with incredible patience as I worked to complete my degree.

My advisor Dr. Bahr deserver's recognition as the mentor who was able to motivate and guide me to believe that no task was too large. Additional guidance and support were provided by my thesis committee Dr. Cill Richards and Dr. Bob Richards.

I would also like to thank Owen Crabtree for his computer modeling and for building the WFT test setup. Julia Martinez provided SEM images and advice with materials related issues. The MEMS group as a whole deserves appreciation for their hard work, training, and all the knowledge gained from working with such a talented group of individuals.

DEVELOPMENT OF A NOVEL METHOD FOR MEASURING THE TRANSVERSE PIEZOELECTRIC COEFFICIENTS OF THIN PIEZOELECTRIC FILMS

Abstract

By Timothy Michael Sullivan, M.S.
Washington State University
August 2004

Chair: David F. Bahr

The transverse piezoelectric properties of thin piezoelectric films were measured using the rectangular membrane method (RMM) developed at Washington State University. This method was compared with other methods from literature performed at WSU. The measured properties were used to evaluate piezoelectric chemistry, processing, poling and substrate conditions. In addition, a alternate generator structure was developed and tested.

Using the RMM it was found that typical values for solution-deposited PZT thin films synthesized at WSU and annealed in a conventional furnace with a titanium to zirconium ratio of 40:60 are an e_{31} of –6.56 C/m^2 and a d_{31} of –76.0 pC/N. These values are for 1 μm thick films poled at 120 kV/cm and aged for 24 hours. The d_{31} value is for a measured PZT Young's modulus of 80 GPa. This is compared with PZT films of 40:60 composition annealed in the RTA. The e_{31} value measured for this film is –4.63 C/m^2. In addition films with he morphotropic phase boundary composition, 52:48, were tested and values of –9.4 C/m^2 and –108.5 pC/N, using the measured 80 GPa Young's modulus, were typical.

TABLE OF CONTENTS

Page

LIST OF TABLES

LIST OF FIGURES

CHAPTER ONE

MOTIVATION

Miniaturization is motivated by reducing weight, power consumption, bulk, and cost. These factors and many others have driven a technology termed microelectromechanical systems (MEMS). This term was coined around 1987 during a series of workshops on microdynamics and MEMS held in Salt Lake City, Utah [1]. This submicron to millimeter [2] scaled technology combines mechanical and electrical components to achieve sensing, actuation, imaging, and even power generation.

The United States Military has interest in micro-scale power generation; particularly fuel flexible devices that have higher power densities and longer lifetimes than currently available batteries. Work being done at Washington State University is using piezoelectric materials to accomplish these goals. In order to achieve high power densities the piezoelectric properties must be maximized.

Piezoelectricity is a phenomenon that occurs in some crystal structures where a surface charge is generated in response to applied stress [3], and conversely the generation of stress in the material in response to an applied surface charge. This phenomenon was first observed by Pierre and Jacques Curie in 1880, and has since been used for transducers, actuators, igniters, micro power generation, and many other devices.

A MEMS scale power generation device is under development at Washington State University, called the P^3 micro engine [4], for Palouse Piezoelectric Power. This device uses an external heat source to expand a two-phase fluid trapped between two thin membranes. One of the membranes is the generator, shown in figure 1.1, which converts

membrane strain into electricity. When the fluid in the cavity is heated, the liquid vaporizes and the membranes bulge due to the expansion of the fluid, converting from the liquid to the vapor phase. The membrane will then come into contact with another membrane in a stack, through the use of a thermal switch [5], and transfer the heat to the next engine in the stack, causing the vapor to condense back to a liquid and the pressure in the cavity to decrease. This event will take place in a cycle at the resonant frequency of the device [6].

Figure 1.1. Photograph of a completed P^3 micro generator.

The piezoelectric properties of the thin films used in the P^3 generator are of great interest to be able to measure changes and advancements in material performance. Existing methods and a new novel approach to testing the piezoelectric properties will be investigated. The new approach, the Rectangular Membrane Method (RMM), will be evaluated and validated through the use of the other established methods. Further, the effects of time after poling and alternative generator geometries will be evaluated.

CHAPTER TWO

PIEZOELECTRICITY AND ITS USE IN A MICRO GENERATOR

The generator membrane consists of a piezoelectric layer between two electrodes, which produces a surface charge as a result of the applied membrane stress, and conversely strains the membrane in response to a surface charge. The ability to quantify the piezoelectric's ability to convert stress and strain into charge is very important for understanding and improving the generator performance. This conversion is measured using the piezoelectric coefficients d_{ij}, and e_{ij}. The transverse piezoelectric properties, d_{31} and e_{31}, are of interest to this work since the two-dimensional modular architecture [4] of the generator utilizes these geometric parameters to produce charge.

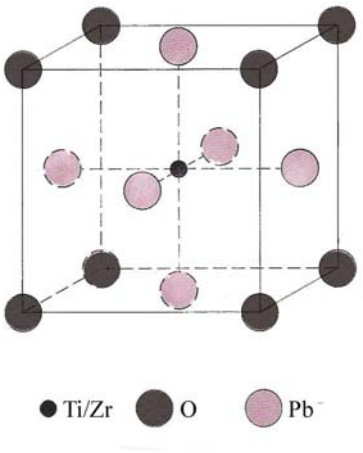

Fig. 2.1. The Perovskite crystal structure [7]

2.1. Fundamentals of Piezoelectricity

Lead zirconate titanate $PbZr_{1-x}Ti_xO_3$ (PZT) is the piezoelectric material used in this study because of its excellent piezoelectric properties. PZT has the desired perovskite structure ABO_3 [7], shown in figure 2.1, in cubic, tetragonal, and

rhombohedral forms, depending on the temperature and composition [8]. However only the non-cubic forms exhibit piezoelectric behavior and are of interest to this study. PZT also exhibits ferroelectric properties; it has a direction of spontaneous polarization which can be oriented by the application of an electric field, and will remain oriented to some degree when that field is removed, demonstrated in figure 2.2.

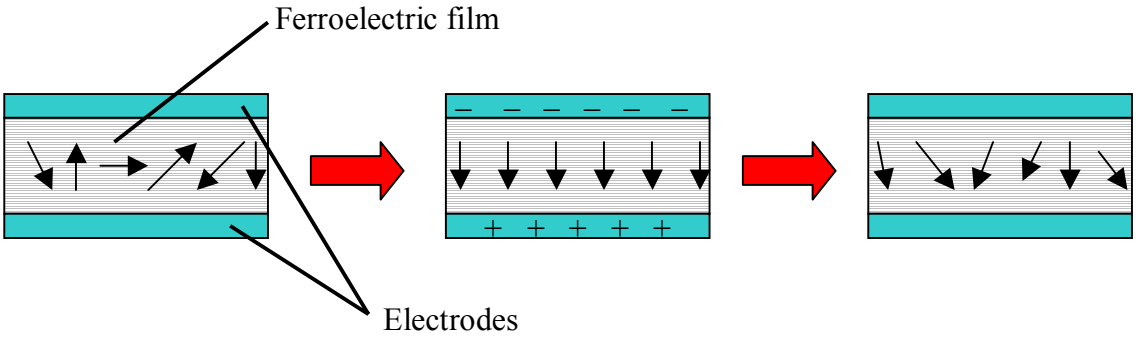

Figure 2.2. Poling of a ferroelectric film by applying an electric field.

Piezoelectric materials can be described using a combination of Gauss' law and Hooke's law to govern the conversion of mechanical energy to electrical energy. These constitutive equations are:

$$S_i = s_{ij}^E T_j + d_{ki} E_k \tag{1}$$

$$D_l = d_{lm} T_m + \varepsilon_{ln}^T E_n \tag{2}$$

where $i,j,m = 1,\ldots,6$ and $k,l,n = 1,2,3$. S, D, E, and T are the strain, dielectric displacement, electric field, and stress, respectively; s_{ij}^E, d_{kl}, and ε_{ln}^T are the elastic compliances, the piezoelectric constants, and the dielectric permitivities [8,9]. The

piezoelectric constants, d_{kl} and e_{kl} are the stress based piezoelectric coefficient with units of $\frac{C}{N}$ and the strain based coefficient with units of $\frac{C}{m^2}$.

The transverse piezoelectric coefficient, d_{31}, defined by IEEE [10] relates the charge produced in the 3 direction to the stress in the 1 direction, as shown in figure 2.3. e_{31} is the strain based transverse piezoelectric coefficient; it relates the charge produced in the 3 direction to the strain in the 1 direction. This is useful because strain can be measured independently of the stress, which requires a knowledge of Young's modulus, which varies significantly among PZT processing methods, and can significantly affect the values of d_{31}.

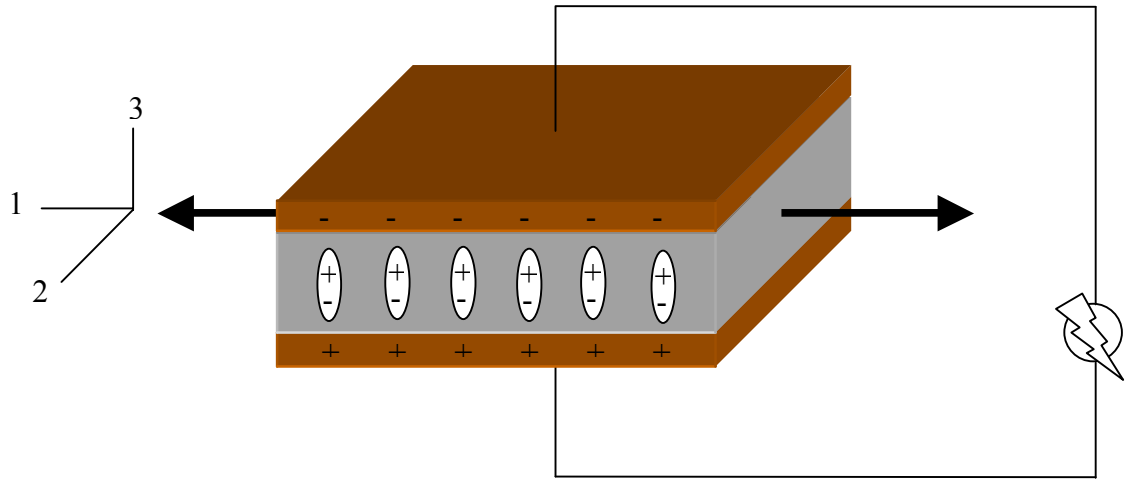

Figure 2.3. Stress in the 1 direction induces a dielectric displacement in the 3 direction.

Piezoelectric coefficients can be measured in a number of ways using either the direct piezoelectric effect, where an induced dielectric displacement is measured as a result of being stressed, or the converse piezoelectric effect, where strain is developed in response to an electric field. Some of the methods used include the normal load method

[11,12,13], the wafer flexure technique (WFT) [14,15], the cantilever method [27,11,16,17], the conversion of electrical field based measurements on square membranes [18], and the rectangular membrane method (RMM), described in chapter four. The RMM was developed at Washington State University as a novel approach for testing piezoelectric properties of the piezoelectric thin films used in the P^3 generator.

Piezoelectrics take many forms including single crystals, polymers, ceramics, and metal oxides of which the most common are quartz, polyvinylidene fluoride (PVDF), barium titanate ($BaTiO_3$) and lead zirconate titanate (PZT), and zinc oxide, respectively. These piezoelectrics vary significantly in their mechanical and piezoelectric properties.

Quartz was the first piezoelectric to be used in a practical application. Cady built the first piezoelectric resonators out of quartz in 1921 [19]. Quartz is still used today in many oscillators and resonators, such as quarts clocks. It has very low piezoelectric properties, typically the transverse piezoelectric coefficient is -1 pC/N [22].

PVDF is a unique piezoelectric in that it is a carbon-based polymer. It is typically spun onto a substrate using a dilute solution in which PVDF powder has been dissolved [22]. Applications of PVDF include high strain bimorphs because of its ability to resist cracking. Another nice feature of PVDF is that it can be purchased in prefabricated sheets complete with electrodes. These sheets can be cut to the desired shape and glued to the substrate. Typical transverse piezoelectric coefficients exhibited by PVDF are -25 pC/N, as will be seen in section 5.1.

Commonly used ceramic piezoelectrics include $BaTiO_3$ and PZT. These piezoelectrics are best known for their high piezoelectric coefficients, with a transverse piezoelectric coefficient of -80 pC/N for $BaTiO_3$ and -110 pC/N for PZT [22]. Because

of these high piezoelectric coefficients, these are typically used in sensing and power generation applications. These films can be sputtered or solution deposited using solvents such as 2Methoxyethanol or Acetic acid.

ZnO can also be sputtered onto the substrate which makes it a commonly used piezoelectric as well. This is typically done by sputtering pure Zn in a O_2/Ar plasma which forms ZnO. The result is a polycrystalline film with its c-axis perpendicular to the surface of the substrate [22]. ZnO has a d_{33} value of 246 pC/N [20] which is lower than 370 pC/N reported for bulk PZT with a high relative permittivity [21].

2.2. Design of P^3 Generator

The generator is the focus of this research. It consists of a two-micron membrane anisotropically etched in the (100) silicon substrate, using a boron doped p-type layer as an etch stop. The pattern is defined by a 100 nm thick low temperature oxide layer grown (wet) then patterned using contact photolithography. Buffered oxide etch (BOE) [22] is used to etch the exposed oxide. This acts as a pattern for the anisotropic ethylene diamine pyrocatechol (EDP) etch [22, p 219], which etches the silicon down to the boron-doped region. A bottom electrode consisting of a 12.5 nm Ti layer and 175 nm Pt is sputtered on the oxide. Lead zirconate titanate (PZT) is deposited on top of the Pt layer using a solution deposition technique [23]. A top electrode made up of a 5 nm TiW adhesion layer and 300 nm of Au is deposited on top. This gold layer is patterned, using contact photolithography, and etched using gold etchant type TFA [22, p 97], leaving only the desired electrode. The PZT is patterned with contact photolithography and the exposed PZT is etched away, using a dilute HF and HCl acid solution, exposing the

bottom electrode and removing excess PZT in the high stress regions of the membrane [24]. The completed structure is shown in figure 2.4.

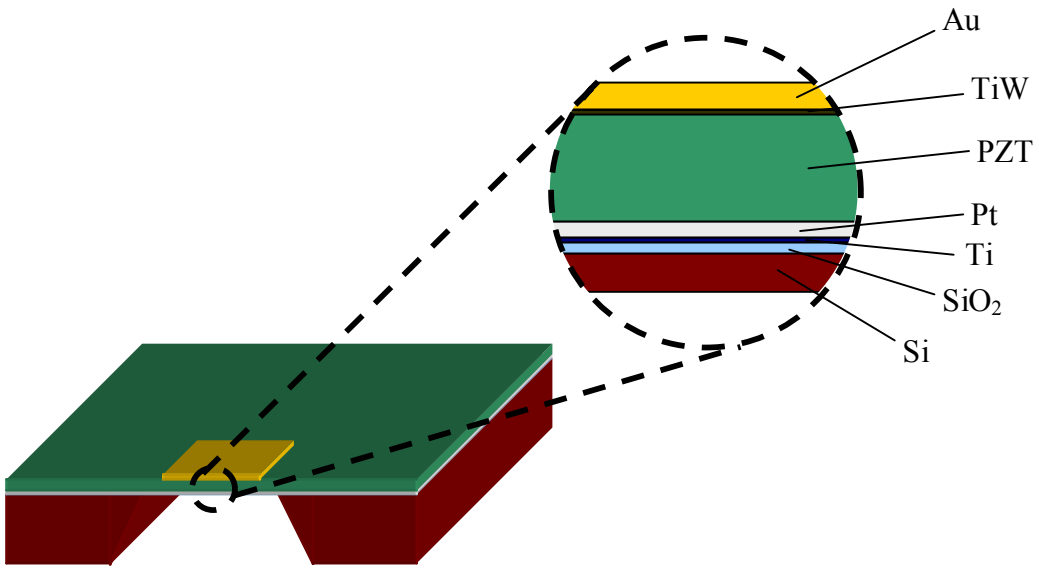

Figure 2.4. Structure of the P^3 generator

A method to quantify how well these generators convert strain energy to electric energy was previously developed at Washington State University [18]. This measure of performance is called specific voltage (SV). It is carried out by mechanically bulging the generator membrane using a bulge tester [25]. This device uses a piezoelectric actuator attached to a diaphragm to pressurize a chamber of water. The generator is mounted over an orifice to the chamber, causing the membrane to bulge when the chamber is pressurized. The generator is bulged sinusiodaly and the pressure and output voltage from the generator are measured using an oscilloscope. Interferograms are captured when the membrane is at its peak deflection. With the center deflection known the percent strain at the center of the membrane can be calculated by

$$\%\varepsilon = \frac{.57h^2}{a^2} \cdot 100 \tag{3}$$

where h is the center deflection, and a is half the side length [26]. Specific voltage can then be represented as

$$SV = \frac{V_{pk-pk}}{\varepsilon\% \cdot t_{PZT}} \tag{4}$$

where $V_{pk\text{-}pk}$ is the peak-to-peak output voltage, and t is the piezoelectric thickness

Specific voltage has served as a good method to evaluate and compare generator performance from wafer to wafer. However, it does not work well for reporting values in publications and for comparing PZT synthesized at WSU with others piezoelectric thin films. That is why a method must be developed which utilizes identical processing to measure the piezoelectric properties. The main focus is on the transverse piezoelectric coefficients, d_{31} and e_{31}.

The current version of the P^3 generator is a 3 X 3 mm membrane, which does not lend itself well to making piezoelectric property measurements. For a given deflection the strain in a square membrane varies large amounts depending on the location on the membrane. The effect of the corners produce a non-uniform stress field, shown in figure 2.5, which is difficult to find the average value. Using a finite difference method computer model the average stress was calculated and compared to the value calculated for the center of the membrane [30]. For a 3 X 3 mm membrane deflected 30 microns, the biaxial center strain was 5% higher than the biaxial strain averaged for the PZT underneath the electrode. This variation will change depending on the magnitude of the deflection so it is not practical to use a computer model to solve for the average strain for the membrane in every condition and with the parameters adjusted every time a

processing change is made. An ideal structure is one that has one dimensional uniform stress, such as a cantilever [27]. Micro cantilevers are difficult to manufacture and are not compatible with the WSU standard generator fabrication techniques.

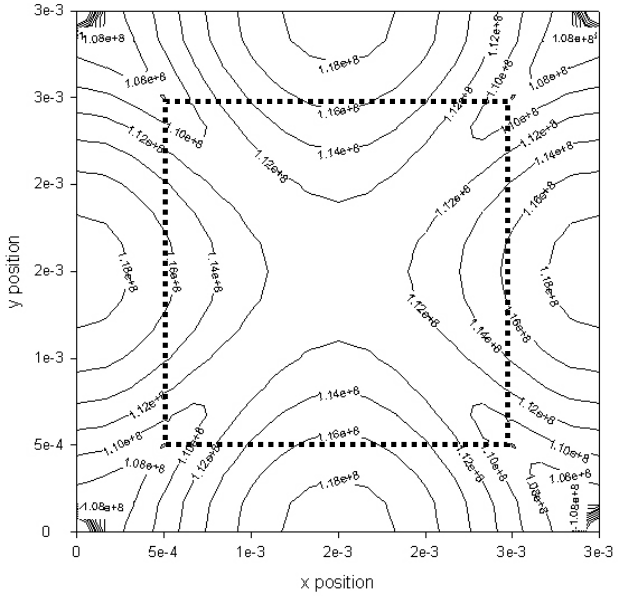

Figure 2.5. Strain distribution plot for a 3x3 mm membrane. The dotted line represents the electrode [30]

Rectangular membranes, on the other hand, can be made using the same processing procedures as standard generators. Rectangular membranes with a side length aspect ratio of four or greater produce in-plane strain deformation at the center of the membrane, with negligible dependence on strain along the longitudinal direction [28]. Since the strain in the longitudinal direction is negligible the strain in the center of the membrane is uniaxial, as shown by Vlassak [28,29]. This can be seen in the strain distribution plot in figure 2.6 [30]. Since rectangular membranes can be produced using the same processing used to produce generators, every generator wafer can have rectangular membrane test structures to evaluate piezoelectric performance. This is

convenient when making changes to the piezoelectric material, whether it is processing or composition changes.

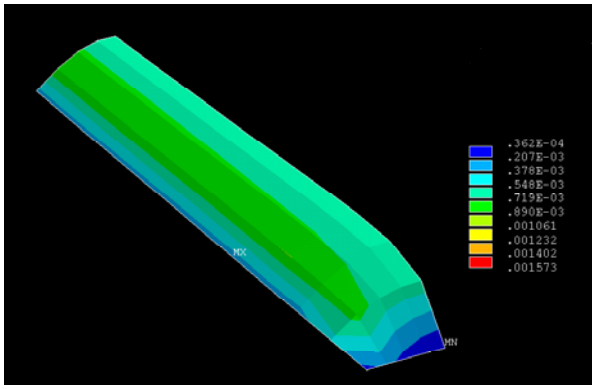

Figure 2.6. Strain field for a 2 X 8 mm rectangular membrane.

CHAPTER THREE

REVIEW OF TESTING METHODS FOR PIEZOELECTRC PROPERTIES

Methods available in the literature for testing the transverse piezoelectric coefficients vary largely depending on which group is testing. Methods range from testing bulk properties [31] to using micro cantilevers [36]. The testing method is often customized to the application of the piezoelectric material. Many of the tests are performed on materials that utilize a solid substrate. This chapter will take an in-depth look at the methods currently used for testing piezoelectric coefficients available in the literature.

3.1. Bulk Testing

Piezoelectric properties on bulk piezoelectrics have been measured in a number of ways. The most common way is to use a Berlincourt d_{33}-meter. This device uses metallic jaws to apply a force on a sample of piezoelectric material and collect the charge produced [31,32]. Another form of this method is to take a cube of piezoelectric material and apply a force on two opposing sides and collect the charge on the sides parallel to the force for the transverse properties or on the surfaces perpendicular to the force for the longitudinal piezoelectric properties, demonstrated in figure 3.1. Thus the piezoelectric coefficients can be calculated by

$$d_{ij} = \frac{Q_j}{F_i} \tag{5}$$

where Q, and F are the charge produced, and the force applied, The area cancels out, since the electrode has the same cross-sectional area as the side with the force applied.

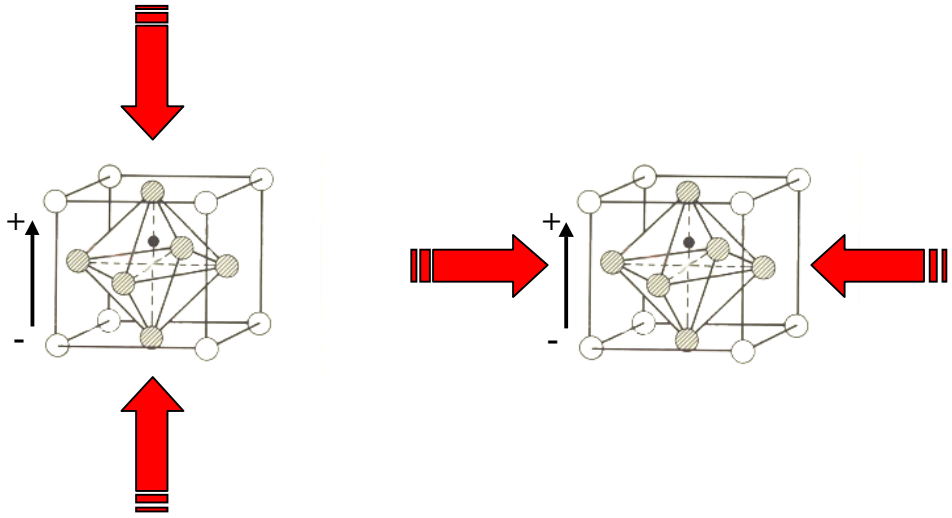

Figure 3.1. Testing of the direct (left) and the transverse (right) piezoelectric coefficients using a Berlincourt meter.

Another method common to bulk piezoelectrics is the laser interferometry method [33, 34], which utilizes the converse piezoelectric effect. Using this method the piezoelectric is subjected to an applied field and the displacement of the piezoelectric is measured using an interferometer. The interferometer uses constructive and destructive interference patterns produced on a sample resulting from out of plane deflection, to measure the magnitude of this deflection. From this method the piezoelectric coefficients can be calculated as

$$d_{ij} = \frac{d_{0,j}}{U_i} \cdot \frac{t}{x} \tag{6}$$

where d_0, t, U, and x are the displacement amplitude, the sample thickness in the direction of the applied field, the driving voltage amplitude, and the corresponding length in the direction of sample deformation, respectively [33].

These methods were intended for testing the properties of bulk piezoelectrics. They have been adapted to thin films, but not very well. The simple force method does

not work for measuring the transverse properties on thin films because the electrodes cannot be mounted on the sides of a thin film. In addition, many thin piezoelectric films are used over membranes, which would break if subjected to metal clamps.

The interferometric methods have been adapted to thin films, however the method becomes much more difficult because the deflections decrease from roughly 10^{-4} m for bulk to less than 10^{-9} m for thin films. This decrease in deflection makes it necessary to have much more sensitive equipment. Double-beam interferometers are used rather than single-beam systems so that unwanted sample movement can be erased from the measurements [11,40]

3.2. Inteferometric Method for Thin Films

As mentioned above, the interferometric method was used for testing bulk properties and was adapted for the use on thin films. This method utilizes the converse piezoelectric effect [35,36], by using a Mach-Zehnder interferometer combined with a phase sensitive amplifier to measure very small vertical displacements as a field is applied to a piezoelectric bimorph. In one study [36], these bimorphs were made up of a 0.44 μm PZT layer sandwiched between two platinum electrodes on a silicon nitride/silicon substrate (0.7/14.3 μm thick), with a 0.9 μm SiO_2 passivation layer. The beam dimensions were 800 and 1000 μm long and 200 μm wide.

A range of bias voltages (up to 6 V) were applied to the bimorph and the relation of tip deflection as a function of bias voltage was obtained and expressed as

$$\delta(L) = \frac{-3d_{31}s_{11}^{Si}s_{11}^{p}t_{Si}\left(t_{Si}+t_{p}\right)L^{2}}{K}V \qquad (7)$$

where s_{11}^{Si} and s_{11}^{p} are the compliance under the mechanical stress of the substrate and the PZT film, respectively, t_{Si} being the thickness of the substrate, t_p that of the PZT film, and

$$K = 4s_{11}^{p}s_{11}^{Si}t_{Si}(t_p)^3 + 4s_{11}^{p}s_{11}^{Si}(t_{Si})^3 t_p + (s_{11}^{p})^2(t_{Si})^4 + (s_{11}^{Si})^2(t_p)^4 + 6s_{11}^{p}s_{11}^{Si}(t_{Si})^2(t_p)^2 \qquad (8)$$

Using the deflection equation above, the authors related the bias voltage to the deflection and used the slope from the linear fit to calculate d_{31}. The following elastic constants were used: Si substrate $s_{11}^{Si} = 0.77\times10^{-11} m^2 N^{-1}$, PZT film, $s_{11}^{p} = 13.8\times10^{-12} m^2 N^{-1}$ (value for bulk ceramic PZT of morphotropic boundary composition, modulus of ~72.5 GPa).

This method is complex because of the sample fabrication, the highly sensitive measurement equipment, and the initial deflected condition of the cantilevers. The methods used to create the cantilevers were not discussed, but most micro cantilevers require complex sacrificial release structures and dry etching procedures to fabricate [22]. To accurately measure the cantilever deflection a Mach-Zehnder interferometer with a resolution on the order of magnitude of 10^{-12} m [36] was used in the experiments. For reference the Michaelson interferometer used at WSU has a resolution on the order of magnitude of 10^{-7} m. Due to the poling induced during plasma etching and residual stress of the PZT the cantilevers were initially deflected. This initial deflection was accounted for in the calculations.

This method is not well suited for testing the piezoelectric films used in the P^3 generator because of the sample fabrication and the small strains are not representative of the generators operating conditions. Properties at large strains are of most interest.

Because of the complex fabrication and experimental setup this method will not be carried out in the current study.

3.3. Wafer Flexure Technique and Adoption at WSU

The wafer flexure technique (WFT) [14] was specifically developed to test the properties of thin films. This method uses the direct effect by bulging an entire wafer to stress the piezoelectric film. This method is not compatible with membranes since the entire wafer must flex. Due to the similar processing this method will be investigated. The samples are fabricated using a platinized silicon wafer with 0.5 molar 52:48 PZT solution deposited using the solution deposition technique. These films were annealed using rapid thermal annealing at 650 ^{0}C for 60 s, resulting in a 0.4 μm thick film. A top electrode of unknown composition was deposited on top and patterned to form electrodes.

To adapt this method at WSU this method uses a specifically designed test sample consisting of a 3", (100) silicon wafer as the substrate. A 12.5 nm thick Ti adhesion layer and then a 175 nm thick Pt layer are sputtered on to make up the bottom electrode. The piezoelectric film was spun on using a solution deposition technique. A 300 nm thick Au top electrode was sputtered on using a 5 nm TiW layer to promote adhesion. The Au layer was patterned with contact photolithography using the mask shown in figure 3.2 and etched, using gold etchant type TFA [22], to form electrodes.

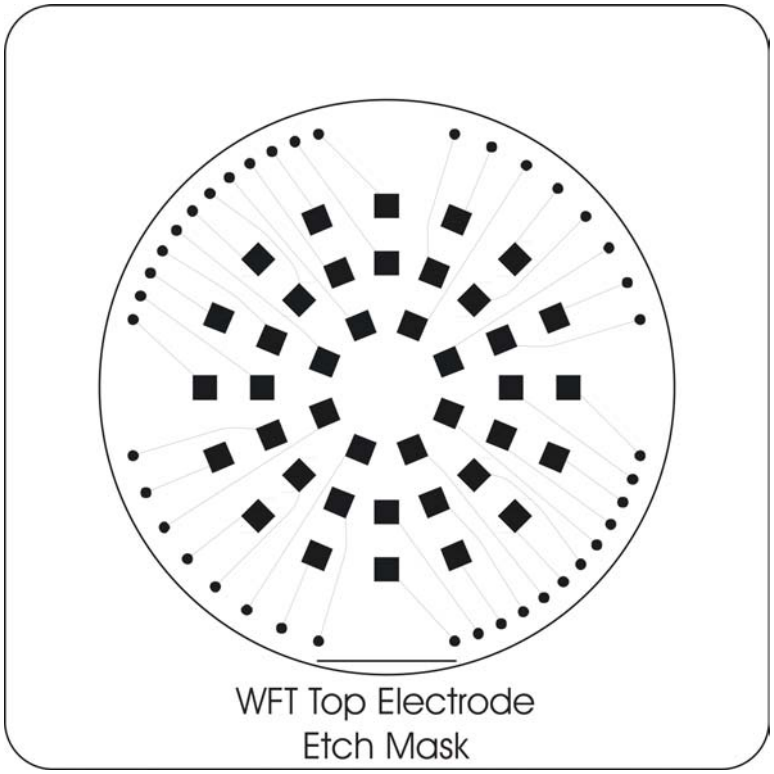

Figure 3.2. Top electrode mask used to pattern wafer flexure technique sample.

The finished wafer is clamped in the test fixture [15], shown in figure 3.3, and pressure is applied to one side of the wafer using nitrogen gas and a pressure regulator. The pressure supply is cut off and the pressure is released rapidly. This change in pressure causes the wafer to go from the bulged state to the initially undeflected state, which relieves the stress in the piezoelectric film. This change in stress produces a charge in the piezoelectric, which is measured using an integrating charge circuit connected to an oscilloscope. The bending stresses, in terms of the radial and tangential components, resulting from the uniform pressure applied to the wafer are [37]:

$$\sigma_r = \frac{3p_0 z}{4t^3}\left[(1-\nu)\rho^2 - (3+\nu)r^2\right] \tag{9}$$

$$\sigma_t = \frac{3p_0 z}{4t^3}\left[(1+\nu)\rho^2 - (1+3\nu)r^2\right] \tag{10}$$

where p_o, z, t, ν, ρ, and r, are the pressure applied to the wafer, the distance from the neutral axis, the film thickness, Poisson's ratio, the support radius, and the distance from the center of the plate, respectively.

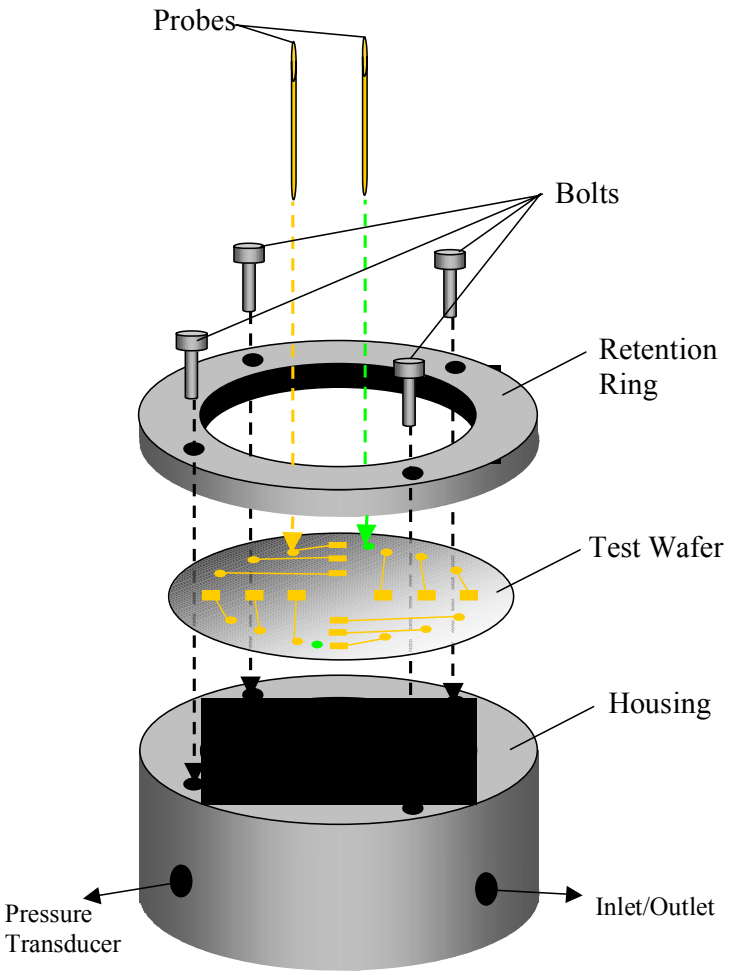

Figure 3.3. Experimental setup used to perform the wafer flexure technique.[14]

Because the silicon and the PZT have different mechanical properties, the plate stresses must be corrected to determine the film stress. Through the use of Hooke's law and by treating σ_t and σ_r as σ_1 and σ_2, the principal strains can be calculated as

$$\varepsilon_1^{Si} = \frac{\sigma_1^{Si}}{E_{Si}} - \nu_{Si}\frac{\sigma_2^{Si}}{E_{si}} \tag{11}$$

$$\varepsilon_2^{Si} = \frac{\sigma_2^{Si}}{E_{Si}} - \nu_{Si}\frac{\sigma_1^{Si}}{E_{si}} \tag{12}$$

where E_{si}, and ν_{si} are Young's modulus and Poisson's ratio for silicon. Because the strain is transferred directly from the substrate to the film the film strain can be calculated as

$$\varepsilon_1^{PZT} = \frac{\sigma_1^{PZT}}{E_{PZT}} - \nu_{PZT}\frac{\sigma_2^{PZT}}{E_{PZT}} \tag{13}$$

$$\varepsilon_2^{PZT} = \frac{\sigma_2^{PZT}}{E_{PZT}} - \nu_{PZT}\frac{\sigma_1^{PZT}}{E_{PZT}} \tag{14}$$

where σ_1^{PZT} and σ_2^{PZT} are

$$\sigma_1^{PZT} = \varepsilon_1^{Si} E_{PZT} + \nu_{PZT}\sigma_2^{PZT} \tag{15}$$

$$\sigma_2^{PZT} = \frac{E_{PZT}}{\left(1-\nu_{PZT}^2\right)}\left(\varepsilon_2^{Si} + \nu_{PZT}\varepsilon_1^{Si}\right) \tag{16}$$

and expanding equation 16 the fundamental form of the equation can be seen in terms of the elastic properties of the silicon and the PZT film

$$\sigma_2^{PZT} = \frac{E_{PZT}}{\left(1-\nu_{PZT}^2\right)}\left[\frac{\sigma_1^{Si}}{E_{Si}}\left(\nu_{PZT}-\nu_{Si}\right) + \frac{\sigma_2^{Si}}{E_{Si}}\left(1-\nu_{PZT}\nu_{Si}\right)\right] \tag{17}$$

and substituting this equation in to equation 15, σ_1^{PZT} becomes

$$\sigma_1^{PZT} = \varepsilon_1^{Si} E_{PZT} + \nu_{PZT}\frac{E_{PZT}}{\left(1-\nu_{PZT}^2\right)}\left[\frac{\sigma_1^{Si}}{E_{Si}}\left(\nu_{PZT}-\nu_{Si}\right) + \frac{\sigma_2^{Si}}{E_{Si}}\left(1-\nu_{PZT}\nu_{Si}\right)\right] \tag{18}$$

These equations hold true for small deflections only, on the order of 20% of the wafer thickness [14]. Larger deflections result in membrane stretching which will lead to

error in the calculations. These principal stresses can be related to the induced dielectric displacement, D_3 (C/m^2) and the piezoelectric coefficient can be calculated as

$$d_{31} = \frac{D_3}{(\sigma_1 + \sigma_2)} \tag{19}$$

This method works well for testing films on solid substrates [14,15,48]. However its major shortfalls are that the test sample is separate from the basic device developed at WSU and that it can only be performed on solid substrates. Having the test sample separate from the device requires the fabrication of a specific test wafer, which is not practical when making frequent changes to processes and the piezoelectric chemistry. Another complication is that piezoelectric coefficients have to be resolved from convoluted two dimensional stress contributions. The fact that this method only works for solid substrates means that the values measured may be inconsistent with the values measured using the RMM. The heating rates and the way that the PZT solution deposits upon the wafer may be different on a solid substrate than on membranes, these slight variations could lead to differences in the piezoelectric properties.

In addition, the equations used in this study to calculate the piezoelectric coefficients rely on Young's modulus of the film. The value chosen greatly affects the amount of stress and strain calculated which changes the piezoelectric coefficients. A value of 101 GPa, which is considered high, was chosen by the authors [14] because it will produce lower bound calculated values. The modulus will change as a result of processing and chemistry changes, so to simply input a constant modulus value into the calculations is not a good representation of the true material properties. The modulus of the PZT film can be measured based on pressure deflection measurements of generator membranes [38] or through the use of nanoindentation [39], however for the sake of

comparison to the values in the literature a value of 101 GPa [14] will be used in this current study.

This value is high compared to the measured value around 80 GPa [38]. Using a large value provides a lower bound for d_{31} values. This can be seen by evaluating equation 17, outlined above. The stress is calculated by multiplying by the modulus of the PZT, so a higher modulus increases the stress calculated for a given charge output. This decreases the ratio of charge to stress which reduces d_{31}.

Properties at large strains are of interest for this study. The P^3 generator will operate at deflections of about 30 μm, which results in a membrane strain of $6x10^{-4}$ at the center of the membrane. It is important to understand the properties at this range. It has been reported that at large strains the force might partially depole the sample (or even damage it), which would decrease the piezoelectric properties [40]. Properties in the large strain region are of interest and need be tested.

3.4 Cantilever Method and Adoption at WSU

Due to the simple nature of bulk cantilevers with thin piezoelectric films, cantilevers are commonly used to measure piezoelectric properties [27,11,16,17]. Dubois and Muralt fabricated cantilevers by dicing wafers with piezoelectric thin films, sandwiched between patterned electrodes, into $15 \times 1.5 \times 0.5$ mm beams, shown in figure 3.4. These beams were dynamically excited by a piezoelectric actuator in contact with the free end, shown in figure 3.5. The output from the piezoelectric was fed through a charge amplifier and the signal was measured using an oscilloscope.

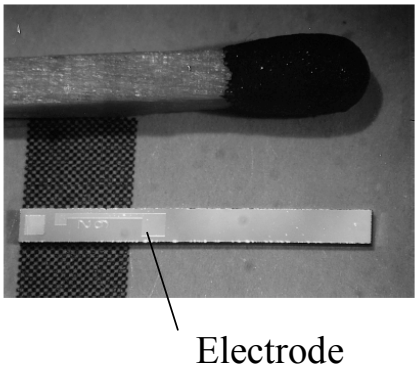

Figure 3.4. Cantilever used by Dubois and Muralt. [27]

In these experiments the strain in the cantilevers was calculated using equations developed by Timoshenko [26], and related to the constitutive equations [41] to calculate the piezoelectric coefficients. The equation linking the transverse piezoelectric coefficient, the electric charge and the displacement of the end of the cantilever is thus:

$$e_{31,f} = \frac{2l^3 Q}{3wtz_l(1-\nu_c)\left(l(x_1 - x_0) - \left(x_1^2 - x_0^2\right)/2\right)} \tag{20}$$

where l, Q, w, t, z, x_1 and x_2 are the length, the charge developed, the width, the thickness, the displacement, the electrode width, and the electrode length, respectively.

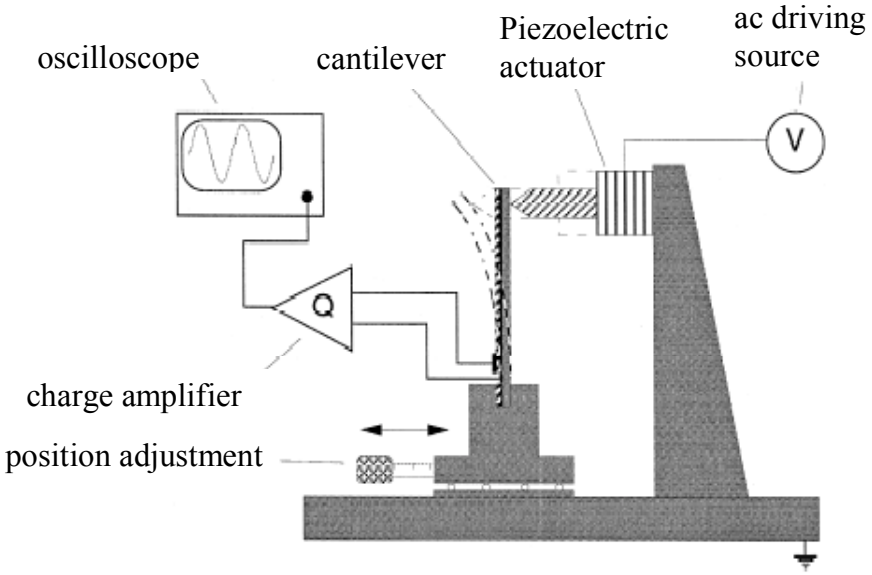

Figure 3.5. Cantilever set-up for measuring piezoelectric properties [27]

This cantilever method could be done using the same fabrication as the wafer flexure technique. It can also be performed using the center portion of the wafer used to produce the P^3 generator. For this reason a variation of the technique will be conducted and the results will be used to compare with the other methods. The center portion of the e_{31} testing wafer has gold patterned with 2 X 2 mm electrodes, as shown in figure 3.6, which are used to characterize the yield of the wafers. This portion can be diced from the wafer, but since dicing was performed by hand the sections are much larger, 2×3 cm, and the edges are not perfectly straight.

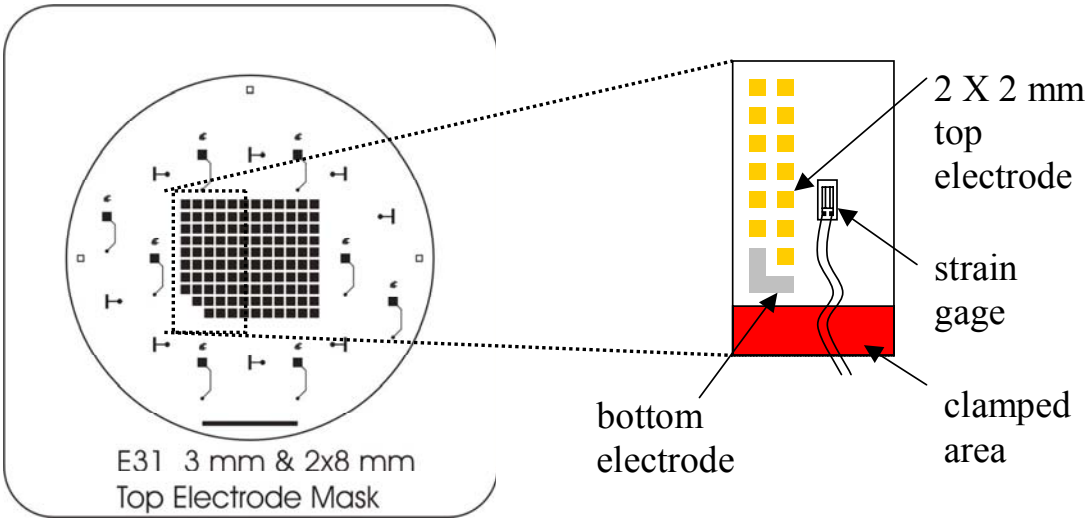

Figure 3.6. Cantilever sample from the center portion of wafer.

Since the cantilevers dimensions varied due to the dicing, strain gauges were used to measure the strain rather than simply using beam theory. EA-06-125BT-120 Micro Measurements strain gages were used and mounted according to the manufactures specifications [42]. The strain gages were mounted parallel and even with the center of

the electrode. A clamp was used to hold one end of the cantilever and the other end was deflected using a micrometer.

An integrating charge circuit (ICC), described in chapter four, was used to measure the charge produced in the piezoelectric. The initial and final strain gage resistance was measured using a four bridge setup on a six digit bench top multimeter. Strain was calculated using

$$\varepsilon = \frac{\Delta R}{R_0 \cdot G} \tag{21}$$

where ΔR, R_0, and G are the change in resistance, initial resistance, and the gage factor, respectively. The strain based piezoelectric coefficient was calculated by

$$e_{31} = \frac{Q}{\varepsilon A} \tag{22}$$

where Q is the charge, ε is the strain, and A is the electrode area. The strain based value can be multiplied by Young's modulus of the PZT as seen in equation 23 to get d_{31}.

$$d_{31} = e_{31} \cdot E_{PZT} \tag{23}$$

This method will be used to compare values with those measured using the rectangular membrane method. This serves multiple purposes; one, to validate that the RMM is measuring the correct values and two, to compare the effect of substrate conditions on the piezoelectric properties. This is because the test pads used in the cantilever method are on a solid silicon substrate where the RMM uses a silicon membrane. Processing conditions may lead to differences in properties between the films on solid substrates and the films on membranes. This is of interest because it is another reason why the piezoelectric properties should be measured using a structure that represents the device.

3.5 Specific Voltage Testing

A method for characterizing the performance of the P^3 generator was developed by Bennet Olson [23]. This method uses a field based measurement called specific voltage (SV). The field produced from the generator when dynamically driven is compared with the strain produced at the center of the 3 X 3 mm generator structure as

$$SV = \frac{V_{pk-pk}}{\varepsilon\% \cdot t_{PZT}} \tag{24}$$

where, V_{pk-pk}, $\varepsilon\%$, and t_{PZT} are the peak-to-peak output voltage, the percent strain at the center of the membrane and the PZT thickness in microns, respectively. The peak-to-peak voltage is read from an oscilloscope and the percent strain is calculated by

$$\varepsilon\% = \frac{.57 \cdot h_0^2}{a^2} \cdot 100 \tag{25}$$

where, h_0 is the center deflection in microns and a is half the side length in microns [26]. SV provides a nondimensionalized way to compare P^3 generators but it is not accepted universally as a way to measure piezoelectric properties. Methods for converting the SV into accepted forms of piezoelectric properties have been developed.

Field based piezoelectric coefficients g_{31} and h_{31} [18] can be used to evaluate piezoelectric performance. Specifically, g_{ij} is the piezoelectric constant relating the electric field produced by a mechanical stress. This can be expressed as

$$g = \frac{\text{open circuit electric field}}{\text{applied mechanical stress}} \tag{26}$$

with the units volts/meter per Newtons/square meter. Likewise, h_{ij} can be expressed as

$$h = \frac{\text{open circuit electric field}}{\text{strain}} \tag{27}$$

with the units volts/meter per meter/meter [43]. SV is roughly equivalent to two times h_{31}. This is true because in a square membrane the stress at the center is produced from strain along both of the membrane axis. So the SV can be related to h_{31} by

$$h_{31} \approx \frac{SV}{2} \tag{28}$$

These values provide a lower bound value for the coefficients because the strain at the center of the membrane is used in the calculation. This strain is higher than the mean strain under the electrode, so by dividing the output by the high strain a lower bound is obtained.

These field-based values are used when the specific voltage is known to get the charge-based piezoelectric coefficients. Conversion is performed using the dielectric constant of the piezoelectric film, k^T. This is a function of the capacitance, electrode area, and thickness of the film, represented by

$$k^T = \frac{Ct}{A} \tag{29}$$

where C, t, and A are the capacitance, thickness, and electrode area, respectively. The capacitance is measured using an HP 4192A impedance analyzer at a frequency of 200 Hz to match the frequency at which SV is measured. This dielectric constant and h_{31} are related to e_{31} as

$$e_{31} = h_{31} k^T \tag{30}$$

Through the use of the SV measurement from a square membrane the strain based piezoelectric coefficient can be calculated. Values obtained using this method will be evaluated and compared to other methods in section 4.4.

CHAPTER FOUR

RECTANGULAR MEMBRANE METHOD

Methods for measuring piezoelectric properties of bulk piezoelectric materials have been established since piezoelectrics were discovered [44]. However, many of these methods do not work for thin films. The Rectangular membrane method (RMM) was developed to accomplish this task. It is important that the films being tested are representative of the films used in the desired application. For the case of the P^3 generator, a method that matched the fabrication and operating conditions did not exist.

4.1. Introduction to the RMM

The RMM is performed on rectangular membranes that are processed in parallel with generator membranes. These rectangular membranes are fabricated using the same steps described in appendix A. The only difference is the mask set used for the contact lithography. This mask set contains an oxide etch mask shown in figure 4.1, a top electrode etch mask shown in figure 4.2, and a bottom electrode etch mask shown in figure 4.3. From this mask set the wafer contains eight square 3 X 3 mm generator membranes and eight rectangular 2 X 8 mm membranes. This pattern was chosen so that the piezoelectric properties measured using the rectangular membranes could be compared with the specific voltage (SV) measured from the square membranes, and a way to convert from SV to e_{31} could be established as discussed in Section 3.5.

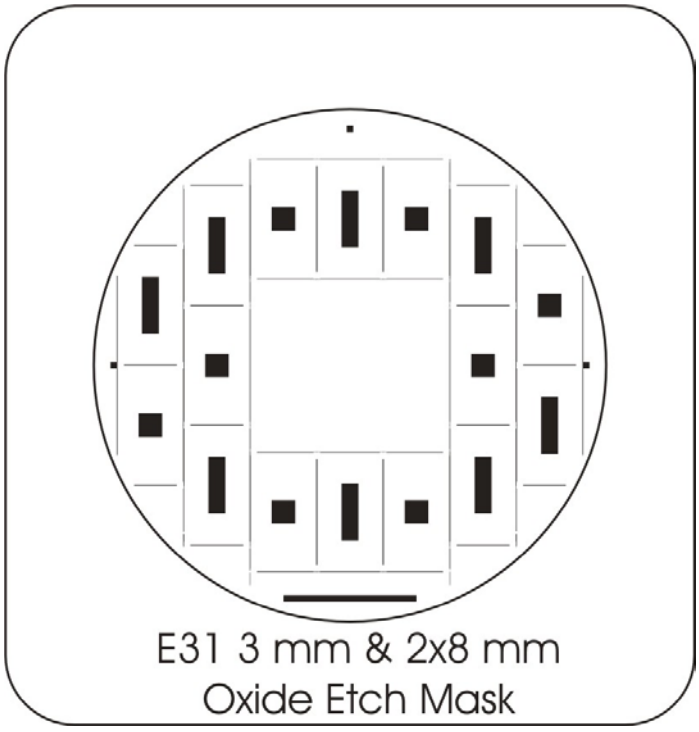

Figure 4.1. Oxide etch mask used to pattern the anisotropic etch.

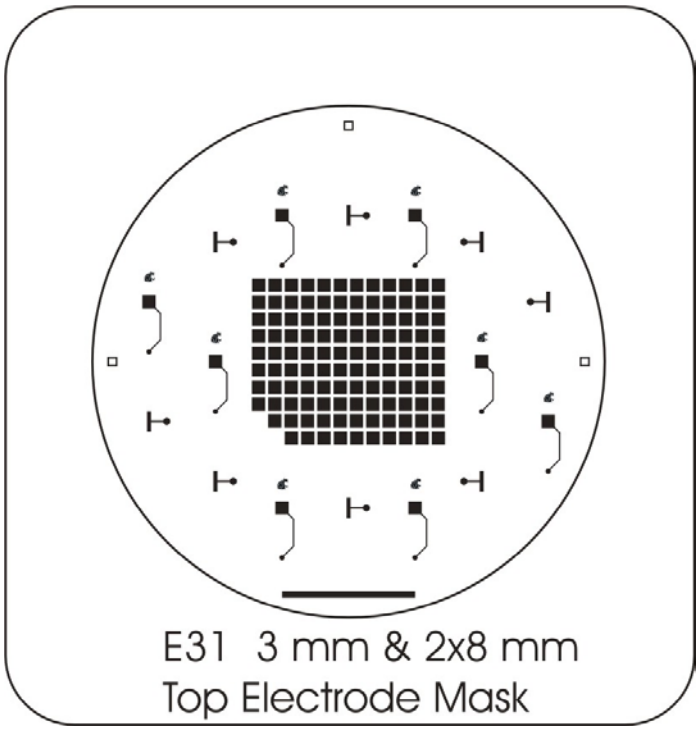

Figure 4.2. Top electrode mask used to pattern the gold etch

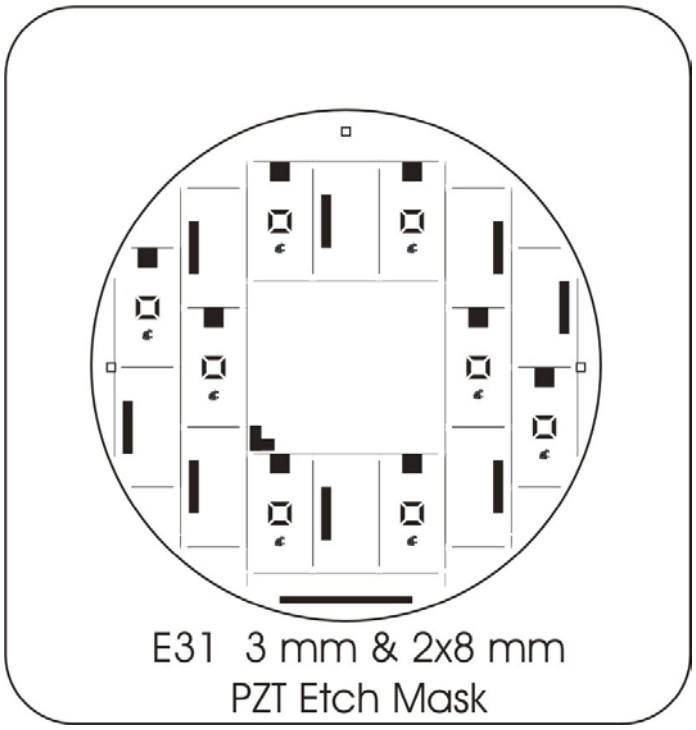

Figure 4.3. Bottom electrode mask used to pattern the PZT etch exposing the bottom electrode.

Rectangular structures were used to measure the piezoelectric constant because the stress at the center of the membrane can easily be calculated based on the center deflection [28,29,45,46]. Since the rectangles have an aspect ratio, *b:a*, of four or greater the stress at the center of the membrane is considered to be one-dimensional [29]. This makes calculating the piezoelectric properties simple and accurate, since there are no complex stress distributions to account for.

The method is performed by measuring the charge produced, using an integrating charge circuit, as the membrane is released from a strained state and returns to its initial state. The ICC outputs a voltage signal, shown in figure 4.4, to an oscilloscope. The magnitude of the voltage output is multiplied by the capacitance of the reference capacitor selected on the ICC, to get the charge. This is represented as

$$Q = C_{REF} V \tag{31}$$

where C_{REF} is the capacitance of the reference capacitor selected and V is the output voltage read from the oscilloscope. From this charge the induced dielectric displacement, D, with units of C/m^2 can be represented as

$$D = \frac{Q}{A} \tag{32}$$

where A is the electrode area.

Before the membrane is released an interferogram, similar to the one shown in figure 4.5, is captured which is used to calculate the center deflection of the membrane. This is performed using a Michaelson interferometer. Deflection is calculated by multiplying the number of fringes by half the wavelength of the Nd:YAG laser (.266 μm). From the deflection, the strain at the center of the membrane can be calculated as

$$\varepsilon_1 = \frac{2h_0^2}{3a^2} \tag{33}$$

where h_0, and a are the center deflection and half the short side length. Through the use of the strain equation and Hooke's law $\sigma = \varepsilon E$ [46] the stress at the center of the membrane is given by

$$\sigma_1 = \frac{2E_{PZT} h_0^2}{3(1-\nu^2)a^2} \tag{34}$$

where E_{PZT}, and ν are the Young's modulus and the Poisson's ratio of the PZT. Using the definition of the induced dielectric displacement $D_{31} = d_{31}\sigma_1$, d_{31} can be calculated as

$$\mathrm{d}_{31} = \frac{3}{2}\frac{\mathrm{C}_{\mathrm{REF}}\mathrm{V}\left[\left(1-\nu^2\right)\mathrm{a}^2\right]}{E_{PZT} h^2 A^2} \tag{35}$$

where V and h are the circuit output voltage and the center deflection and C, ν, a, E_{PZT}, and A are the reference capacitance, Poisson's ratio, half the short side length, an estimated Young's modulus of the PZT (101 MPa), and electrode area, respectively. Likewise, e_{31} can be calculated from the dielectric displacement in terms of the strain, $D_{31} = e_{31}\varepsilon_1$, as

$$e_{31} = \frac{3}{2}\frac{C_{REF}Va^2}{h_0^2 A} \tag{36}$$

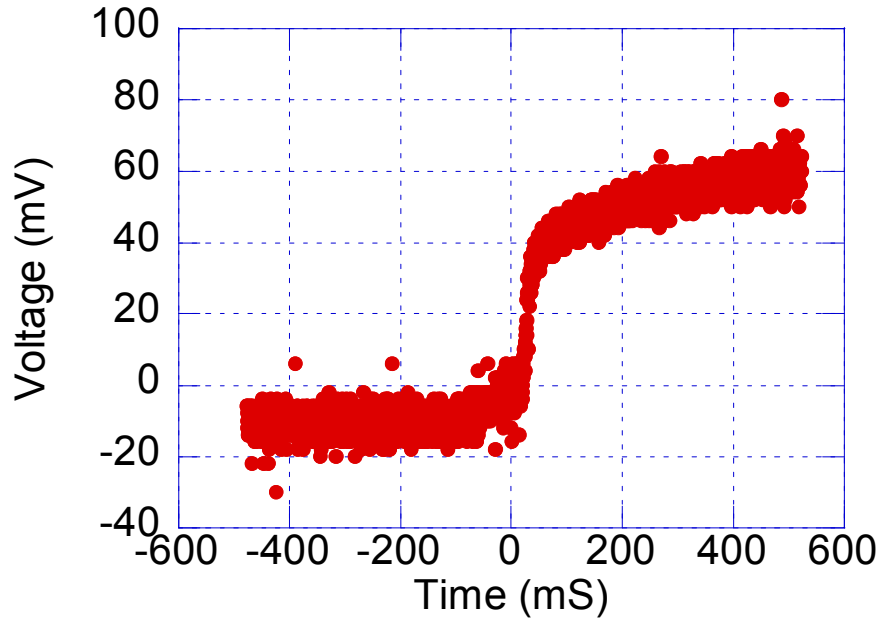

Figure 4.4. Output signal from the integrated charge circuit for a RMM test.

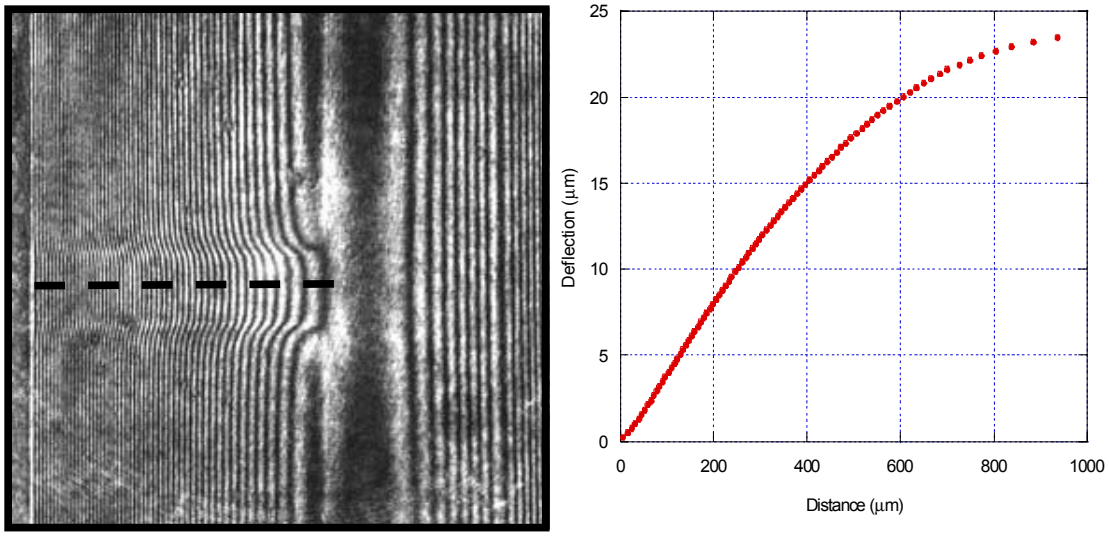

Figure 4.5. The interferogram used to calculate the center deflection. The plot shows the membrane profile corresponding to the interferogram.

The strain based transverse piezoelectric coefficient, e_{31}, is a better measure of piezoelectric performance because it is independent of the Young's modulus of the PZT. 101 MPa was used to calculate d_{31} even though much lower values have been measured [38]. This value was used because it is commonly used in literature [47]. Other values are often used when reporting d_{31}, which affects the magnitude of d_{31} substantially. Since e_{31} is measured independent of the modulus, values can be compared with other reported values without taking into consideration which modulus was used.

4.2. RMM Procedures

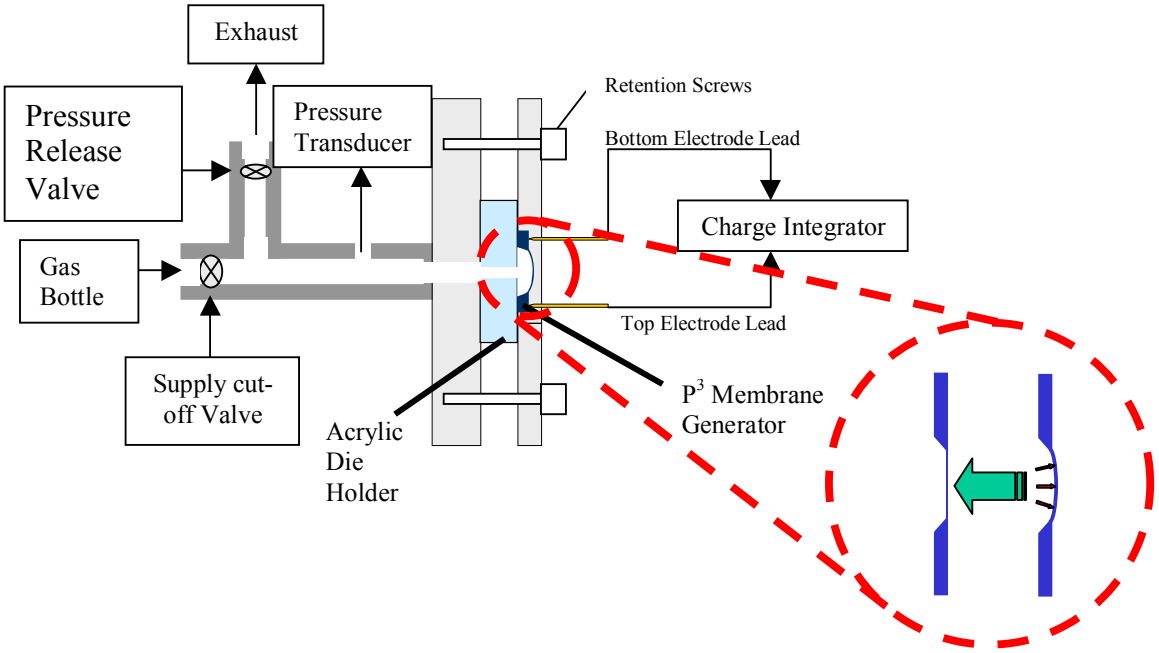

Figure 4.6. Bulge test setup used to perform the RMM.

Produce RMM samples using mask set that includes 2 X 8 mm test die. Dice the wafer along the dicing lines indicated by the lines etched in the piezoelectric on the top of the wafer. Epoxy the rectangular die to an acrylic sample holder. This is a 3/8 inch thick acrylic piece cut to 1.5 X 1.5 inches and has a 1/8 inch hole drilled in the center. Be sure to only epoxy around the edge of the die, to ensure that no epoxy gets inside the membrane cavity, as shown in figure 4.7. (NOTE: run a sharp razor blade over the acrylic surface before applying the epoxy to ensure that the sample holder does not have any obstructions on it. The samples need to be mounted flat). With the epoxy set, the sample is loaded into the static bulge (tail pointed down), as shown in figure 4.6, and should be mounted in front of the interferometer as shown in figure 4.9.

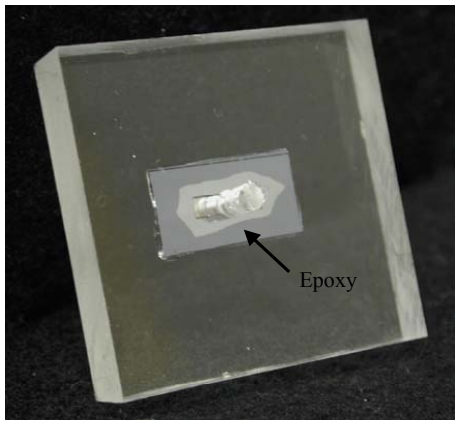

Figure 4.7. Die mounted on acrylic test fixture. The epoxy is only around the edge of the die.

Connect the probes so that they are contacting the electrodes. Use the offset probes to ensure that the cameras view of the membrane is not obstructed. Connect the leads to the integrating charge circuit (ICC), top electrode to the red terminal and bottom electrode to the black terminal. Also connect the ICC to the oscilloscope using a BNC cable. Turn on the ICC and make sure that the correct reference capacitor is selected (Typically 129 nF for standard testing, use 5.15 nF if higher resolution is required). Adjust the ZERO knob until the output signal is at zero when the REFRESH button is pressed. This should be done with the REFRESH button pressed. Make sure that the regulator on the nitrogen tank is backed out far enough so that no nitrogen will flow. Turn on the nitrogen gas at the main valve. Open the supply valve on the static bulge tester and close the release valve, shown in figure 4.6. Tare the pressure transducer, and turn the regulator valve clockwise until set to the desired pressure (less than 3 psi for rectangular membranes).

To operate the interferometer, turn key on laser power supply to ON position, allow laser to warm up for at least 30 minutes. Make sure that the laser settings are as follows: Eof, F10,180, P01, 0.93, Sof. Open **Xcap for windows** software on the control computer. Go to **PIXCI** and select **OPEN/CLOSE,** the **PIXCI OPEN/CLOSE** window will pop up. Make sure that **Multiple Devices** is selected and click the **Open** button. Select the **Capt.** tab and click on the **LIVE** button. Arrange light pointing at the beam splitter so that the membrane electrode appears in view as shown in figure 4.7. If the electrode is not in view manually adjust the sample position until the electrode can be seen. Fine adjustment can be done by adjusting the microscope positioning micrometers.

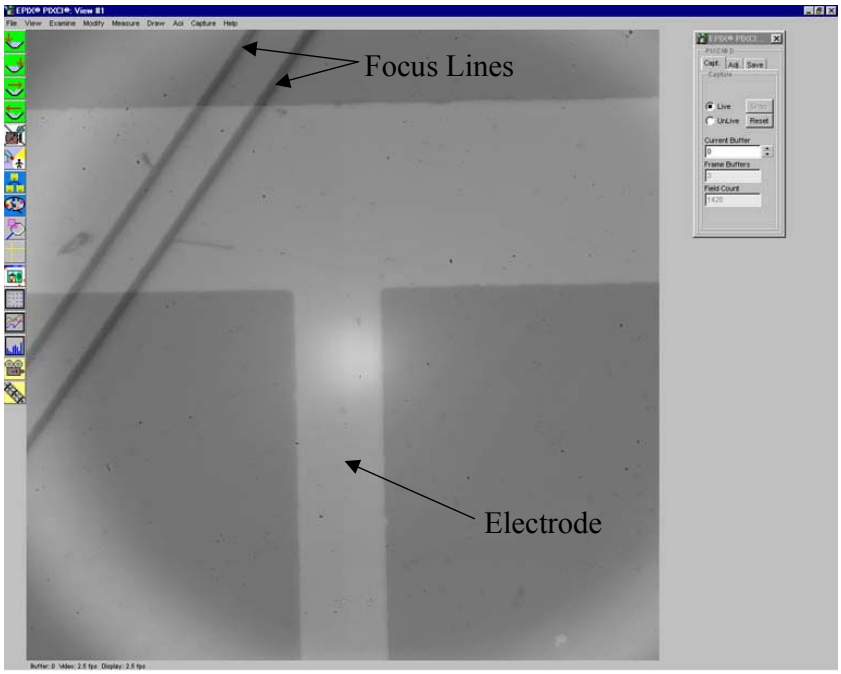

Figure 4.8. Long distance microscope focused on the electrode. The parallel lines indicate that the mirror is also in focus.

Focus the microscope on the electrode using the focusing adjustment on the lens. Focus the mirror by adjusting the positioning wheels until two parallel lines appear in view. Adjust the depth adjustment wheel on the mirror support until these lines are in

focus, as shown in figure 4.7. Move the mirror slightly until these lines are out of view, and remove the positioning light. Push the START button and then the SHUTTER button on the laser power supply (the laser should begin pulsing). Open the manual shutter on the laser. The computer should show the membrane with interference patterns all over, at this stage these will probably be very random. Adjust the mirror plain adjustment screws until the fringes disappear. This occurs when the mirror is orthogonal to the sample. Click on the UNLIVE button to enable manual triggering to capture interferograms.

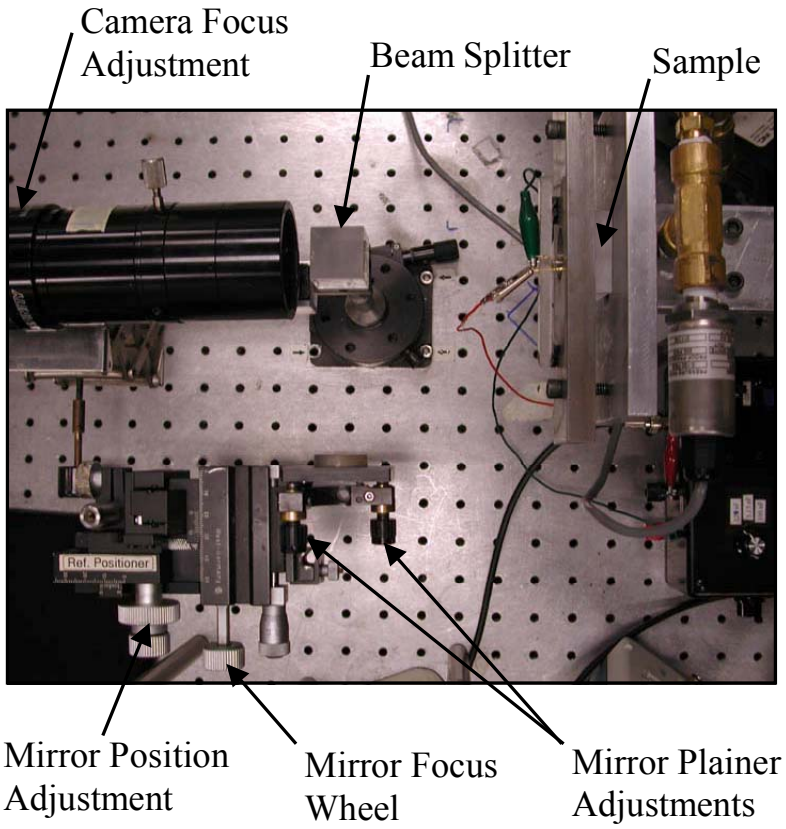

Figure 4.9. Experimental setup showing the sample and the reference mirror.

Apply pressure to the membrane by closing the RELEASE valve and opening the SUPPLY valve. Press the SNAP button to capture the image of the deflected membrane. Repeat as necessary to obtain a clear picture. SAVE the interferogram naming it according to the pressure applied. Hold down the REFRESH button and make sure that the signal is properly zeroed. Release the REFRESH button, close the SUPPLY valve, and open the RELEASE valve, rapidly in that order. Read the output voltage from the signal mean on the oscilloscope and record. Enter the output voltage, the pressure, and the number of fringes into the spreadsheet titled "Piezo Properties.xls" stored on the "shared" drive.

To count the fringes use the FCOUNT program in MatLab as described: Open interferogram using Windows Photo Editor, rotate the image 45^0 so that it appears as shown in figure 4.10, save image and close. Open MatLab 5.3, and type FCOUNT, this will prompt a window to open your file. Select your file, the picture will be displayed in the window. Click on the picture at the center of the electrode, and then click at the edge of the membrane as shown in figure 4.10. This will tell the program where to analyze. The interferogram will now appear with colored lines at the fringes. This indicates that the program counted that fringe. If there are fringes that do not have a colored line add them to the number of fringes output by the program. This number should be input to the spreadsheet. Close the release valve and open the supply valve. Repeat the steps as desired. When done, turn off the main nitrogen supply valve and all other equipment.

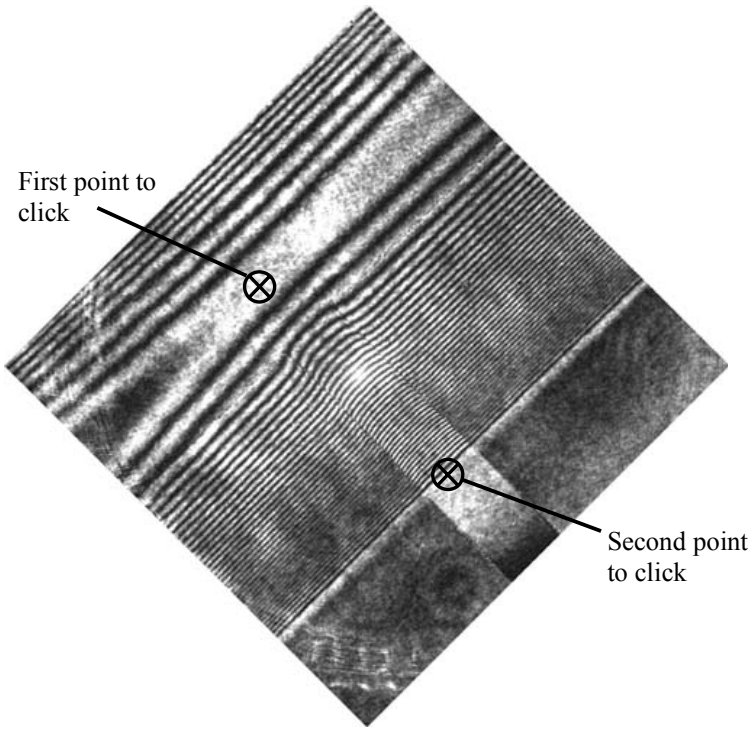

Figure 4.10. Interferogram ready for fringe counter program.

4.3. Integrating Charge Circuit Operation

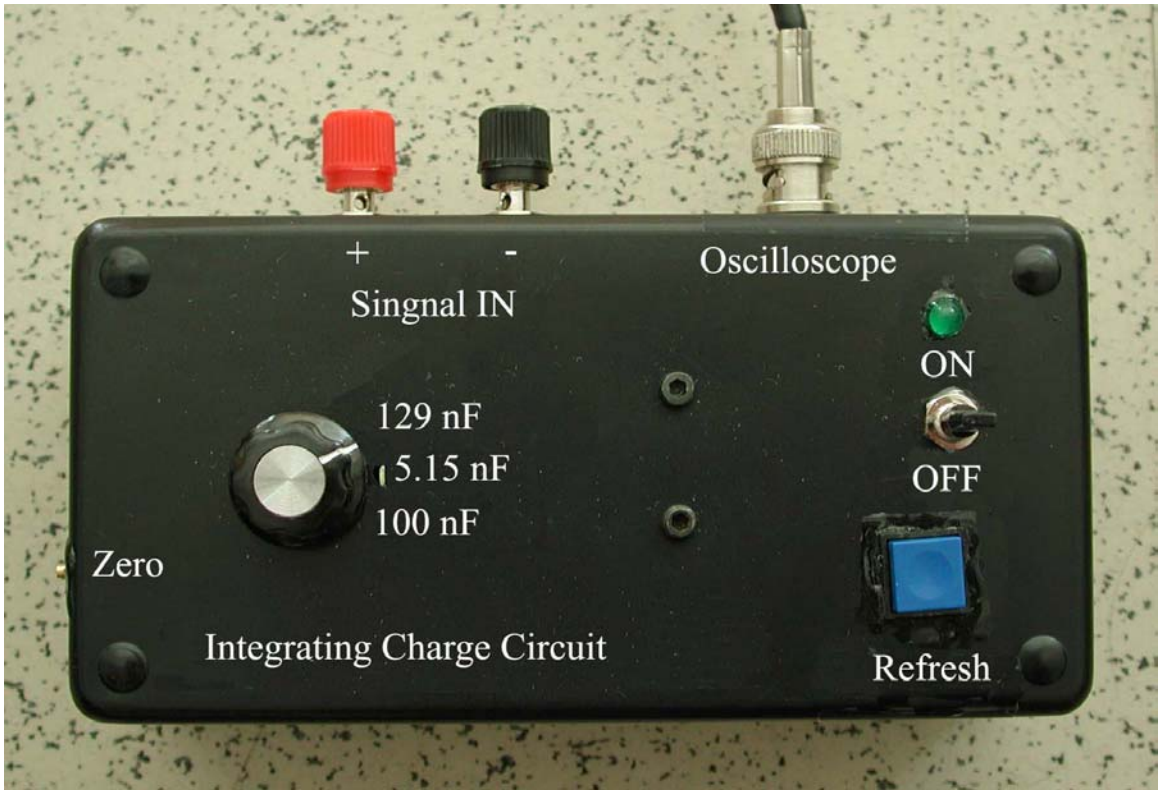

Figure 4.11. Integrating Charge integrating circuit.

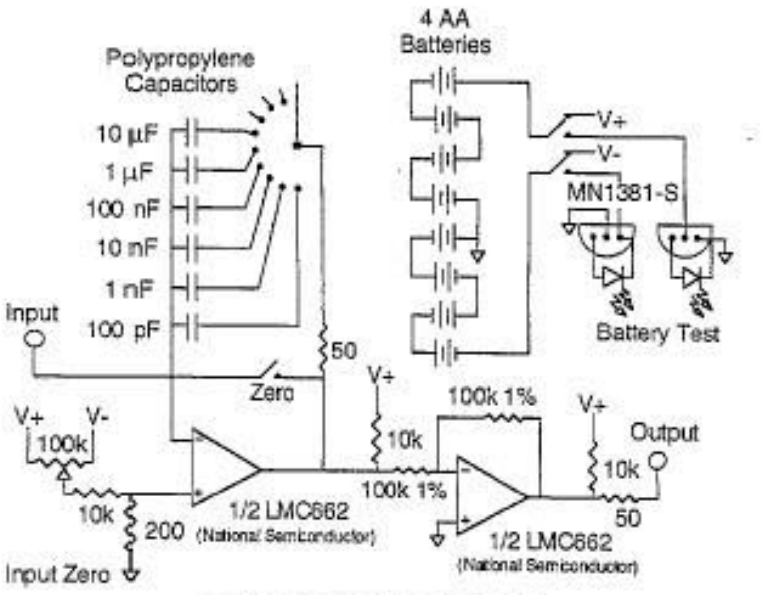

Figure 4.12. Schematic of the circuitry used in the integrating charge circuit.[14]

Attach BNC cable from the output to the input of the oscilloscope. Attach leads from the electrodes to the positive and negative terminals, top electrode to the red terminal and bottom electrode to the black terminal. Turn power switch to the ON position (verify that the LED is glowing green, if it is not check the batteries, located inside the box). Adjust the oscilloscope to DC coupling and to read the signal mean and the appropriate scale to see signal (5-50 mV/div). Press the refresh button and adjust the ZERO knob until the signal is around zero. Press REFRESH button before testing.

The integrating charge circuit used to monitor the films dielectric displacement as a function of mechanical stress is shown in figure 4.12 [14]. Charge produced in the piezoelectric film is fed into an integrating operational amplifier. The charge is collected on a capacitor and then the output voltage is inverted using a second operational amplifier. The output voltage is proportional to the charge stored on the reference capacitor.

To verify that the charge integrating circuit was functioning properly, capacitors were charged using a power supply set to 1 volt and the charge circuit was used to measure the charge stored in the capacitor. As shown in figure 4.13, the measured charge corresponded well to the charge that was input into the circuit, and a slope of 1.068 was found when the measured charge value was plotted versus the input charge. This small amount of error could be attributed to variations in the values of the capacitors from the reported values and variations in the voltage output from the power supply.

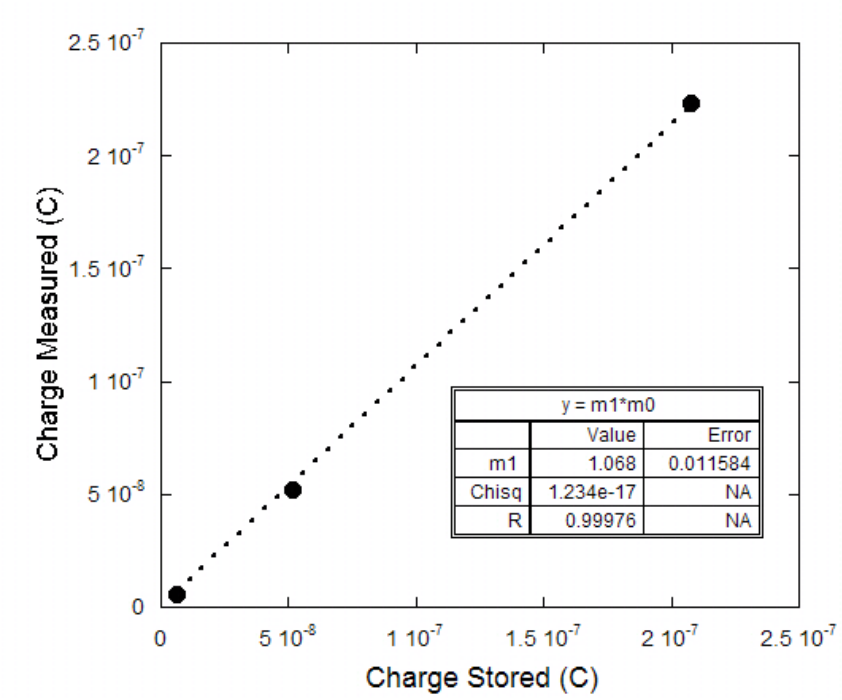

Figure 4.13. Charge stored on capacitors was measured using the integrating charge circuit. Comparing the stored values with the measured values shows the charge circuit is functioning properly.

4.4. Comparison of Specific Voltage Based Measurements to RMM Measurements

Before the RMM was developed evaluation of the P^3 generator was performed using the specific voltage method as discussed in section 3.5. The specific voltage measurements corresponding to past processing and chemistry changes would be more

useful for evaluating future developments if the data was in terms of the piezoelectric coefficients commonly used in the literature. Conversion from specific voltage to e_{31} can be performed using the dielectric constant of the films as demonstrated in section 3.5. This conversion is useful but only possible when the dielectric constant for the film is known. This was not a known when specific voltage was used to evaluate the PZT, so dielectric constant values corresponding to the specific voltage data does not exist in most cases.

The relation between e_{31} calculated from specific voltage and e_{31} measured using the RMM was investigated by comparing measurements from the same wafer. This was done by utilizing the e_{31} wafer design described in section 4.1,which contains both square and rectangular membranes. From these measurements the linear trend relating e_{31} calculated from specific voltage to e_{31} measured using the RMM, shown in figure 4.14, was found. This shows that for films of the 40:60 titanium to zirconium composition the dielectric constant does not vary much from sample to sample and the relation stated in equation 38 can be used to calculate e_{31} for 40:60 films with a known specific voltage when the dielectric constant is unknown.

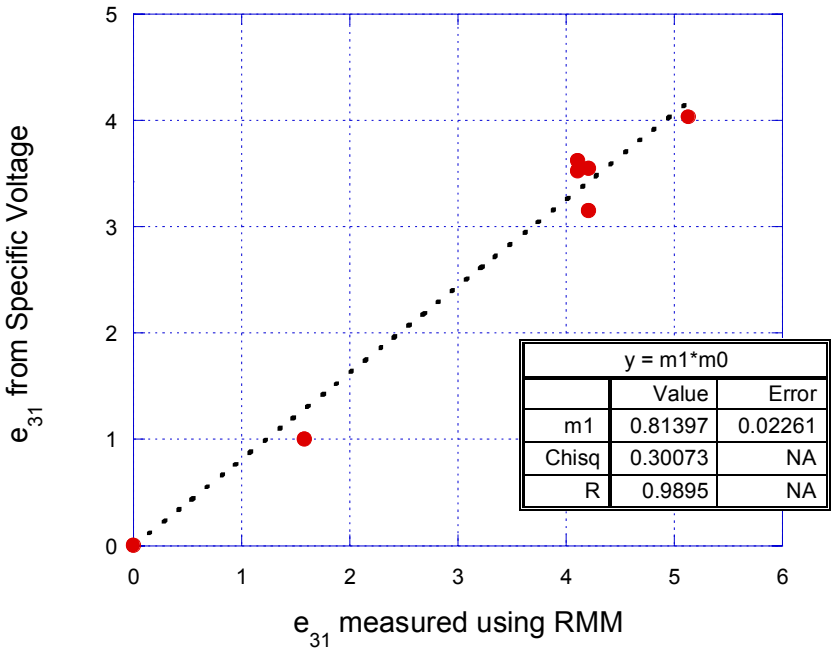

Figure 4.14. Comparison of e_{31} calculated from specific voltage to e_{31} measured using the RMM for 40:60 PZT films. The slope is half the dielectric constant multiplied by 1 X 10^8 to get the proper units.

From the comparison of e_{31} calculated from specific voltage to e_{31} measured using the RMM it is shown that the calculated value is 81% of the measured value. The relation can be expressed as

$$e_{31,SV} = 0.814 e_{31,meas} \tag{37}$$

so calculating e_{31} from specific voltage provides a low-end estimate of e_{31}. Using a finite difference computer model the difference from the measured to the converted e_{31} value was investigated. The model showed that the average strain under the electrode for a 3 X 3 mm membrane is 5% less than the strain at the center of the membrane. Since the strain at the center of the membrane is used to calculate e_{31} this difference would account for 5% of the difference between the converted value and the measured value. Some of the additional difference could be attributed to the experimental error between the two methods. Both methods are performed using different measurement equipment, which

could lead to a bias error when the values are converted. The important factor to note is that when converting specific voltage to e31 the differences between the average strain for a square membrane and the center strain used in the calculation combined with equipment and measurement errors the converted value is a low end value.

Further the relation between specific voltage and e_{31} calculated from specific voltage and dielectric permittivity can be determined by fitting a trend line to the data shown in figure 4.15. It can be seen that the equation

$$e_{31,SV} = .37SV \tag{38}$$

best fits the data for 40:60 PZT.

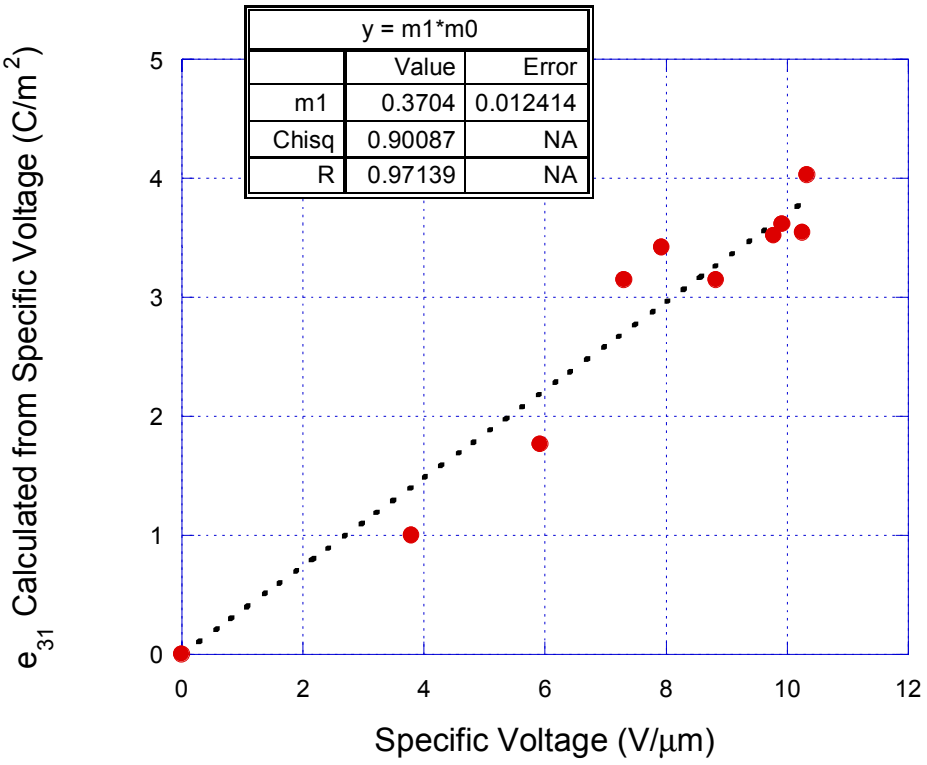

Figure 4.15. Relation between specific voltage and e_{31} calculated from specific voltage. They are related through the dielectric constant of the PZT.

Because the dielectric constant for films with different composition changes these relations only hold true for 40:60 PZT. If other films are used the dielectric constant can be measured and used to relate specific voltage to the lower bound estimate e_{31}. However with the introduction of the RMM this should not be necessary for future testing.

CHAPTER FIVE

VALIDATION OF THE RECTANGULAR MEMBRANE METHOD

5.1 Validation Using Cantilevers

For comparison, a cantilever method was used to further validate the RMM. Cantilevers were constructed using the center portion of the e_{31} wafers. Thus the same sample preparation was used to create them as the rectangular membranes used in the RMM. The center portion of the wafer was diced to achieve a rectangular geometry, as described in section 3.4. 2 X 2 mm electrodes were patterned to harvest the charge. The strain was measured using a Micro-Measurements strain gauge glued directly to the SiO_2 parallel and next to the electrode. This ensured that the strain measured by the strain gauge was the same as the strain under the electrode. The charge was harvested using the integrating charge circuit described in section 4.1. A micrometer was used to deflect the end of the cantilever in a controlled manner.

Values obtained using the RMM are comparable to values measured by other groups using similar PZT [27,14,12,16,48,49,50,51,52,53]. However, the method had not been verified using a piezoelectric with known properties. In order to link the RMM with a piezoelectric of known properties, the cantilever method was employed using PVDF film prepared by Measurement Specialties. PVDF film, 8 X 12.6 mm, was attached to an aluminum cantilever parallel to a Micro-Measurements EA-06-125BT-120 strain gage. The PVDF was attached using Micro-Measurements strain gage adhesive and application technique.

The cantilever was clamped in a holder as shown in figure 5.1, and the end deflected. The strain was measured from the strain gage and the charge was collected

from the PVDF film using an integrating charge circuit connected to an oscilloscope. d_{31} was calculated as follows:

$$d_{31} = \frac{D_3}{E\varepsilon_1} \tag{39}$$

Where D is the charge per unit electrode area, E is Young's Modulus of the film and ε is the strain in the film.

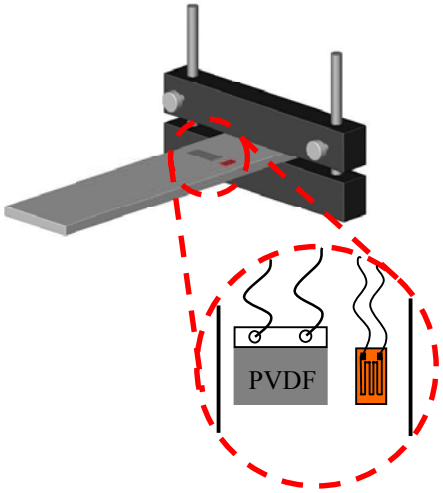

Figure 5.1. PVDF cantilever test setup. The PVDF was mounted parallel to the strain gage.

Using this technique, and the Young's modulus supplied by the manufacturer (3 GPa), the d_{31} of the PVDF film was measured to be –22.5 pC/N. This compares very well with the manufacture's reported value of –23 pC/N. The correlation between these values proves that the cantilever method is a valid method for measuring piezoelectric coefficients.

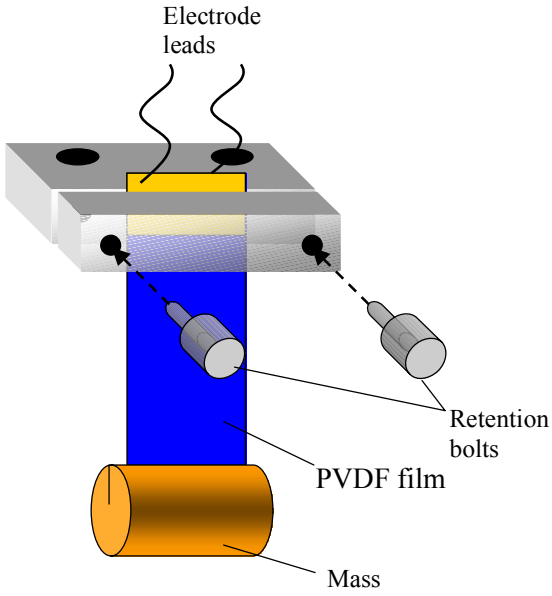

Figure 5.2. Hanging mass method. The mass stresses the film resulting in a charge accumulation on the electrodes.

In addition to comparing the measured d_{31} value for the PVDF film with the manufacturer's reported values, the reported values were tested using the manufacturer's method, the hanging mass method. This method involves supporting the film at one end and hanging a mass from the other, as shown in figure 5.2. The mass is supported and the integrating charge circuit is refreshed then the mass support is removed so that the film supports the mass, stressing the film. The charge produced is measured using the integrating charge circuit. The stress in the film can be calculated using the simple expression

$$\sigma = \frac{Mg}{A} \tag{40}$$

where M, g, and A are the hanging mass, the acceleration of gravity (9.81 m/s^2), and film cross-sectional area, respectively. d_{31} is calculated by comparing the induced dielectric displacement to the membrane stress as

$$d_{31} = \frac{D_3}{\sigma_1} \tag{41}$$

Using this method a d_{31} of –25 pC/N was obtained, which is comparable to the manufacture's value and the value measured using the cantilever method. The agreement in the values measured using the manufactures hanging mass method and the cantilever method can be used to support the cantilever method as a valid method for testing piezoelectric properties, as shown in the flow chart in figure 5.3. The cantilever method will then be compared to the RMM as a way to validate it.

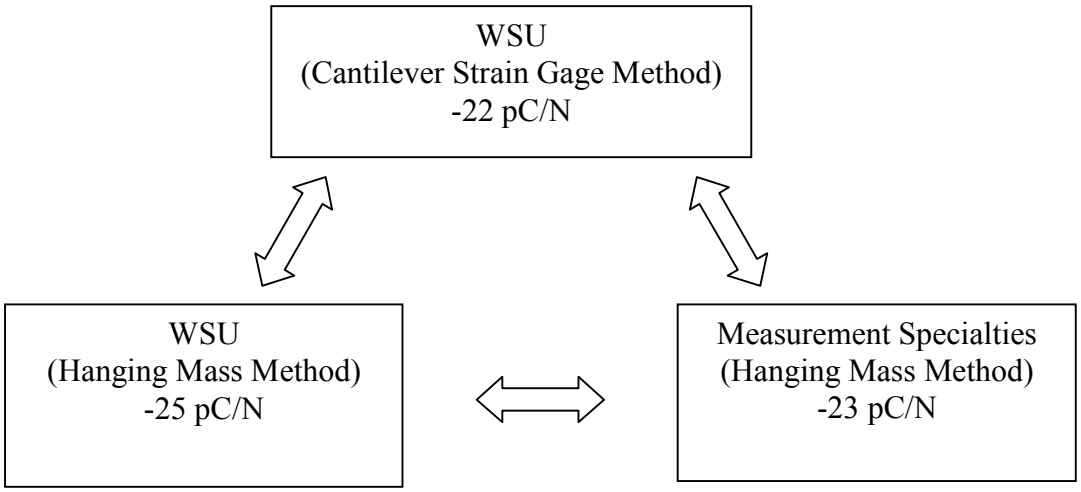

Figure 5.3. Flow chart relating the cantilever validation tests for testing PVDF film.

5.2 Validation of Rectangular Structure

The aluminum cantilevers with PVDF adhered to them and strain gages to measure the film strain was verified using the hanging mass method. Similarly the aluminum cantilevers with PVDF can be used to validate using the center portion of the wafer as a cantilever and using a strain gage to measure the strain. This test was performed as described in section 3.4. The center portion of the wafers were diced into rectangles and mounted with a strain gage, and then one end was clamped. Probes were

used to contact the electrodes. An integrating charge circuit described in section 4.1 was used to collect the charge produced when the cantilever was deflected. The free end of the cantilever was deflected quasistatically using a micrometer. The end was deflected and the resultant strain measured, then the beam was returned to its undeflected state by reversing the micrometer. The charge was collected when the beam was returned to its initial position.

Using this method e_{31} values of -4.38 C/m^2 were measured for 1 μm thick 40:60 PZT poled at 120 kV/cm for 10 minutes and aged 24 hours. This value is very comparable to the value of -4.63 C/m^2 averaged from three membranes tested using the RMM on rectangular membranes from the same wafer with the same poling conditions. This testing path shows that the PVDF testing can be related to the cantilever method performed on the center portions of the wafer which can then be compared to the values obtained using the RMM.

5.3 Validation of In-Plane Strain

Rectangular membranes with an aspect ratio of four were used in this study because the end effect can be ignored [29]. This implies that the PZT is stressed in only the one direction along the axis of the short side. The ends deflect similar to that of a square membrane so the non-uniform strain is at the ends and not the center of the membrane.

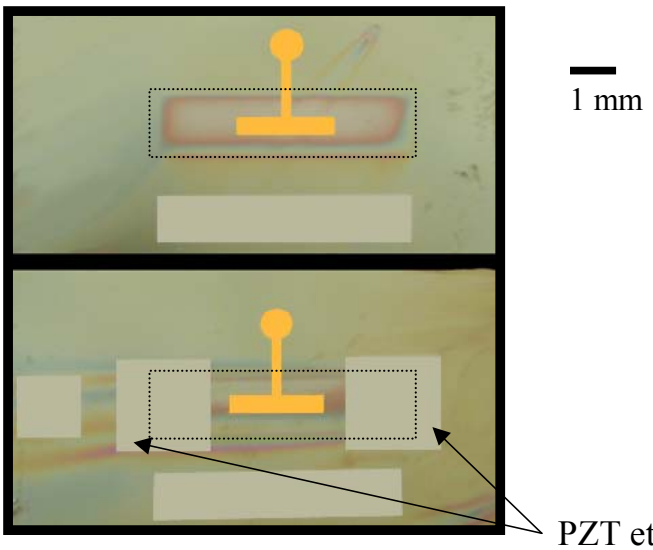

Figure 5.4. Top: Un-etched RMM Sample. Bottom: Etched RMM sample. The dashed rectangles indicate the extent of the membrane.

Tests were performed to determine the effects of the ends of the rectangles and the electrode tail. The PZT at the ends of the rectangles was etched off in the patterns shown in figure 5.4. This was to reduce the stress contribution in the PZT from the longitudinal direction. Pressure deflection data was taken from the die before and after the etching. In figure 5.5 you can see that the etching did not affect the center deflection of the membrane. Since the deflection did not increase it would imply that the ends of the membrane do not contribute significantly to the overall pressure-deflection relationship and the strain in the membrane is controlled by the shortest side. $d_{31}$was compared to another, unpoled, rectangular membrane from the same wafer. These values are very similar, etched (-13.8 pC/N) and unetched (-13.3 pC/N). Unpoled samples were used to ensure that slight variations (ie. aging time and poling voltage) did not affect the evaluation of the pressure deflection or the piezoelectric properties. The strong

correlation between the un-etched and the etched samples indicates that an aspect ratio of four is large enough to completely neglect the stress contributions from the end of the membrane.

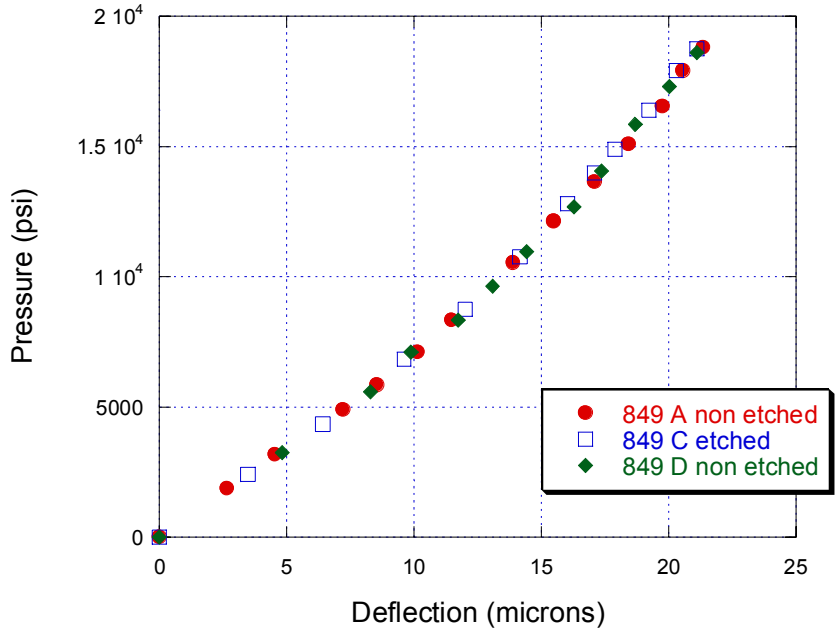

Figure 5.5. Pressure deflection curves comparing the etched membrane to the non-etched membranes. The similarity further indicates that the longitudinal stress is negligible.

The aspect ratio of four was used in this study because the membranes were more robust than ones with larger aspect ratios. 2 X 12 mm membranes were also produced. These membranes broke more frequently in fabrication and testing. This is a serious drawback when wafer space is important and only one or two testing membranes are on each wafer. The 2 X 12 mm membranes took away from the structural rigidity of the die so they were also more prone to buckling when loaded into the testing equipment.

To contact the electrode a "tail" is used so that the electrodes do not interfere with the membrane, shown in figure 5.6. The rectangular main part of the rectangle is 3120 X 580 μm which is equal to an area of 1.82×10^{-6} m^2. The portion of the tail that is on the

membrane is 720 X 275 μm, an area of 1.98×10^{-7} m^2. Comparing these two areas reveals that the tail makes up 11% of the total electrode area subjected to stress. To first order, the electrode tail should contribute 11% of the total magnitude of the piezoelectric coefficients. However, the stress over the tail portion varies due to the bending effect and boundary conditions at the edge of the membrane. It is important to verify that using the total strained portion (rectangle + tail over the membrane) of the electrode to calculate the piezoelectric coefficients is correct.

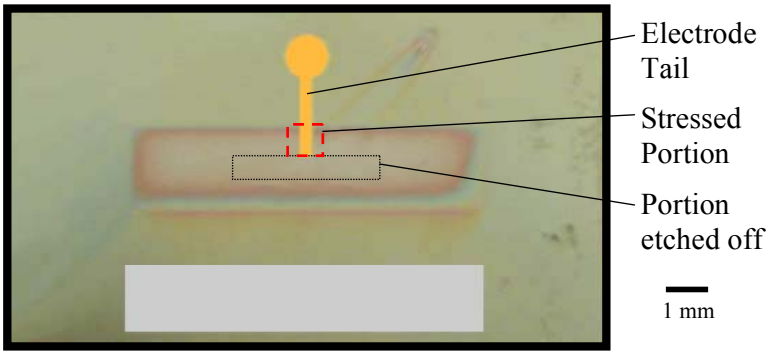

Figure 5.6. Sample with etched electrode used to measure the affect of the electrode tail.

To verify this experimentally, the rectangular portion of the electrode was etched off, as shown in figure 5.6, and the RMM was performed using only the tail portion of the electrode to collect charge. Equation 31 was used to calculate e_{31} resulting in a mean value of -0.55 C/m^2, compared to the mean value of -6.82 C/m^2 for the entire electrode. A comparison of the values measured is shown in figure 5.7. Comparing the values in figure 5.7, it was found that the value measured using only the tail portion was 8% of the total value measured using the entire electrode. This is very close to the tail's portion of the total electrode area. From this experiment it can be concluded that the stress in the PZT under the electrode tail contributing to charge collected by the tail is similar to that

calculated at the center of the membrane and the contribution to the total charge is proportional to the tail's contribution to electrode area. This implies that the tail does not affect the piezoelectric coefficients measured using the RMM.

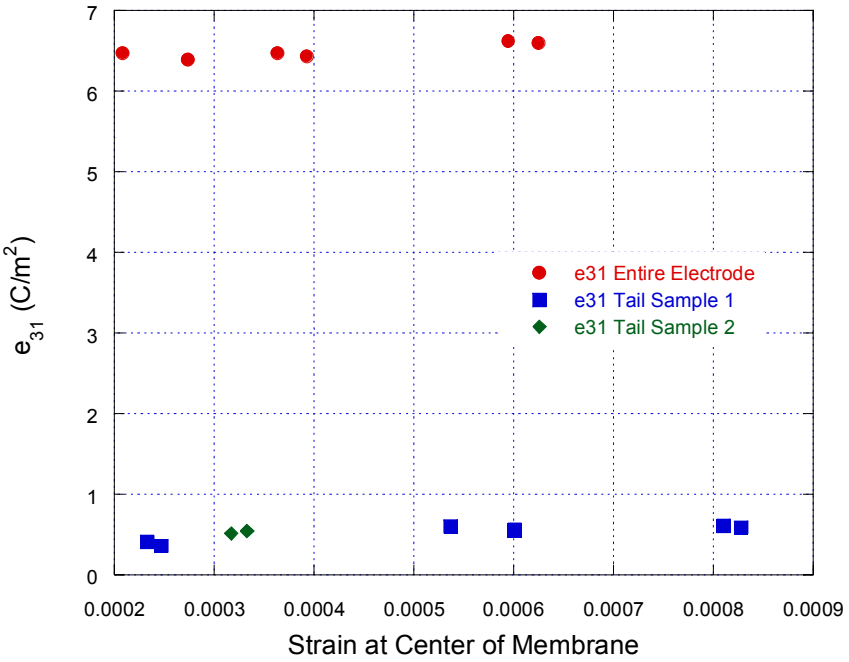

Figure 5.7. Comparison of e_{31} values measured using the electrode tail and the entire electrode for a 1 μm thick 40:60 PZT film.

Another important factor regarding the electrode tail is does it act as a parasitic capacitance that reduces the amount of charge measured? In order to answer this question the measurement system must be analyzed. It is constructed of three parts the area of the electrode that is stressed and produces charge (active electrode), the area of the electrode that is not stressed but still on PZT (inactive electrode), and the integrating charge circuit. Since the active electrode and the inactive electrode are connected they act as parallel capacitors. Therefore the charge produced as a result of the dielectric displacement is distributed over the entire electrode area and the charge is $Q = CV$, where C is proportional to the electrode area. Due to the fact that the amount of charge produced is a function of the piezoelectric coefficient of the PZT and the active electrode

area, as long as the active electrode area does not change the amount of charge produced will not change. If the inactive portion of the electrode increases this charge will be distributed over a larger capacitor but the charge will still remain the same. The integrating charge circuit uses an operational amplifier that has infinite impedance, which serves to isolate the PZT sample capacitance from the reference capacitor in the charge circuit. So no matter what size the inactive electrode area is the charge will simply be distributed over the entire electrode area and measured by the integrating charge circuit. The voltage signal that the charge circuit is input may change but its change is proportional to the change in the electrodes capacitance by $Q=CV$ so the integrating charge circuit will still measure the same amount of charge. The size of the tail portion of the electrode will not affect the measurement of charge produced in the PZT for a given dielectric displacement.

5.4 Validation of Testing Pressure

Since the RMM is not conventional in that it uses large strains to measure the piezoelectric properties it is important to investigate the effects of the large strains. For the purpose of standardizing the RMM, the affect of the applied pressure on the piezoelectric property measurements was investigated. The RMM was performed on a single membrane thirty times. The pressure applied during the test was randomly assigned between .5 and 3 psi. This pressure range was divided into four pressure groups for analysis. These groups being Low, Medium-Low, Medium-High, and High which were .5-.99 psi, 1-1.49 psi, 1.5-1.99 psi, and greater than 2 psi, respectively. Since the order of the test pressures used was randomly chosen from these pressure groups, the number of samples in each group was not equal. To determine if a single-factor ANOVA

[54] test was appropriate, where $H_0 : \overline{d}_{31\,Low} = \overline{d}_{31\,Med-Low} = \overline{d}_{31\,Med-High} = \overline{d}_{31\,High}$ vs. H_a: at least two of the means are different; the residual plots were analyzed to see if the data was normal. Figure 5.8 shows these residual plots, it can be seen that the normal probability plot fits a straight line and does not show any other distinct trends, and that the residuals versus fitted values plots shows that the data all fall within a reasonable range. From this it can be concluded that the data is normal and a single factor ANOVA test is appropriate.

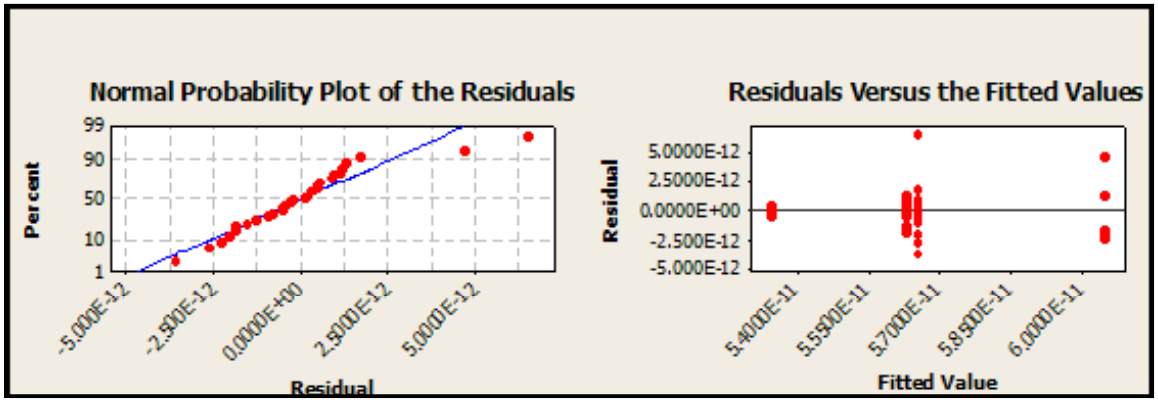

Figure 5.8. Residual plots used to determine normality of the data.

As indicated by the hypothesis to be tested, the mean piezoelectric coefficient for each range is compared to determine if they are equivalent at the 0.05 significance level. From the ANOVA table, calculated using MINITAB [55], a P-value of 0.005 is obtained. This P-value is less than the significance level of 0.05, which indicates that H_0 is rejected in favor of H_a: at least two of the means are different.

Since there are differences between at least two of the means it is important to determine which samples are different. Tukey's method was used to compare the sample means [54]. From this analysis it was determined that $\overline{d}_{31\,Low}$ is significantly different from all the other means.

When testing in the Low pressure range the charge produced in the piezoelectric is small and therefore the signal to noise ratio is also small. This makes it difficult to get accurate measurements and that is why the mean value for the piezoelectric coefficient is significantly different than the values obtained when testing at higher pressures.

From this statistical analysis it can be determined that the RMM should be performed at a pressure differential of two pounds per square inch. The charge produced at this pressure is large enough to get an accurate measurement with the equipment used in this study. The other factor that plays a role in the testing pressure is that ability to resolve the interferograms used to measure the deflection. At a pressure differential of two pounds per square inch the deflection at the center of the 2 x 8 mm membrane is usually on the order of 20 μm, which can be resolved from the interferogram. At higher pressures the interferograms become more difficult to resolve leading to error in calculating the center deflection of the membrane.

5.5 Validation Using the Wafer Flexure Technique

The Wafer Flexure Technique (WFT) [14] was used in this study to further validate the RMM. It was chosen because the same fabrication processes are used to make the WFT samples and the e_{31} testing wafer, except for the pits. An entire 3 inch wafer was used to make the samples and the tests were performed as described in section 3.3.

WFT tests were performed on two test pads on the same wafer and their values were averaged to get a mean e_{31} of –3.57 C/m^2. This value is lower than the –6.56 C/m^2 average for similar 1 μm thick 40:60 PZT films tested using the RMM, but it is still

comparable and would fall within the lower limits of the data. Since membranes cannot exist on the WFT samples a direct comparison could not be performed. The piezoelectric coefficients are consistent for films with the same processing and composition.

The low values could be a result of testing on a solid substrate versus over a membrane. The heating conditions and the spinning conditions can vary from solid substrate to membranes. The membranes do not come in direct contact with the hotplate during the pyrolization step so the heating rate and the flow of heat may be different. When spinning the membranes deflect downward due to the air passing underneath them. This may also affect the piezoelectric properties. So the values measured using these two techniques are comparable to each other and within the same range.

CHAPTER SIX

EFFECT OF CONVENTIONAL ANNEALING VS. RTA, POLING, COMPSITION, AND SUBSTRATE CONDITION

6.1 Conventional Annealing Versus Rapid Thermal Annealing

Solution deposited PZT thin films must go through certain steps in order to achieve tetragonal structure and columnar growth. The PZT solution is spun on the wafer at 3000 rpm for 30 seconds, and then pyrolized at 375 ^{0}C for 2 min. This process is repeated three times and then the wafer is crystallized . Crystallization is performed two different ways. The first is using a conventional tube furnace set to 700 ^{0}C. The wafer is lowered into the furnace over the course of one minute to allow the wafer to heat evenly. Annealing is done for ten minutes and then the wafer is removed from the furnace in a one minute pull. This ten minute process has been reported to increase grain size, resulting in higher domain wall mobility and lower residual stress [56].

Rapid thermal annealing (RTA) can also be used for this process. This process is performed by loading the wafer into a SiC susceptor, and loading the susceptor into the furnace. The furnace ramps up to 700 ^{0}C in 15-20 seconds, 45 ^{0}C/s, then holds the temperature at steady state for 30 seconds, and then is allowed to cool. The rapid ramp up to temperature makes it possible to anneal films in less than a minute rather than the standard 10 minutes in the conventional furnace. This reduction in annealing time reduces the time that out-diffusion has to occur resulting in films with more controlled composition. In addition RTA annealed films demonstrate better surface morphology. However it has been reported that the rapid heating and cooling rates can lead to higher stresses in the film [57].

The mean value from RMM tests performed on six conventionally annealed wafers was compared to the value measured from two wafers annealed using the RTA. This comparison resulted in a mean e_{31} value of –6.56 C/m^2 with a standard deviation of 0.74 C/m^2 for the conventionally annealed films and –5.90 C/m^2 for the films annealed using the RTA. Comparison of the piezoelectric coefficients between solution deposited PZT crystallized in the conventional furnace vs. PZT crystallized in the RTA reveal that the piezoelectric properties on the RTA films were a little lower than the conventionally annealed films. In addition the films processed using the RTA were less compliant, which can be seen from the pressure deflection plots in figure 6.1.

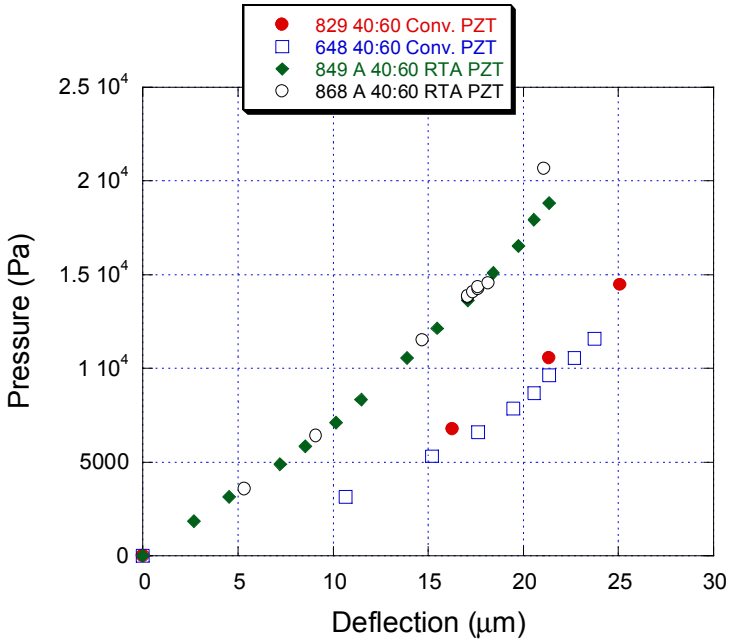

Figure 6.1. Pressure deflection curves for PZT with different processing and chemistry.

Looking at the piezoelectric properties and the decrease in compliance the film annealed using the RTA with a fast ramp and short anneal time would not be well suited for use in the P^3 generator. The compliance plays a significant role in making the generator run efficiently so it is necessary to have a compliant film.

As a caveat to the prior statement the RTA process was not optimized. A short anneal time was used which may not have been long enough for the PZT to fully anneal, resulting in a high stress film. The annealing time should be adjusted to optimize the piezoelectric and mechanical properties, but was not carried out in this study.

6.2 Poling

Lead zirconate titanate is one of the piezoelectric materials that also exhibits ferroelectric behavior[44]. This is an advantage for use in the generator, it allows for the PZT to be polarized using an electric field, which aligns the dipoles. Most bulk piezoelectrics are poled at a temperature around or above their Curie temperature (Tc) [7]. This is the temperature where the crystal is no longer tetragonal in structure but becomes cubic, which is not piezoelectric. Since the focus is on thin films this is not necessary because thin films will orient with just the application of an electric field on the order of two-to-three times the coercive field [15]. When the field is removed some of the dipoles stay oriented making it possible to produce more charge when the PZT is stressed due to the aligned nature of the film. The amount of remnant polarization is a function of time after poling. The effects of poling decrease logarithmically with time [15]. This can be accelerated depending on stress [58] and exposure to UV radiation [59]. Only the effect of time will be investigated in this study.

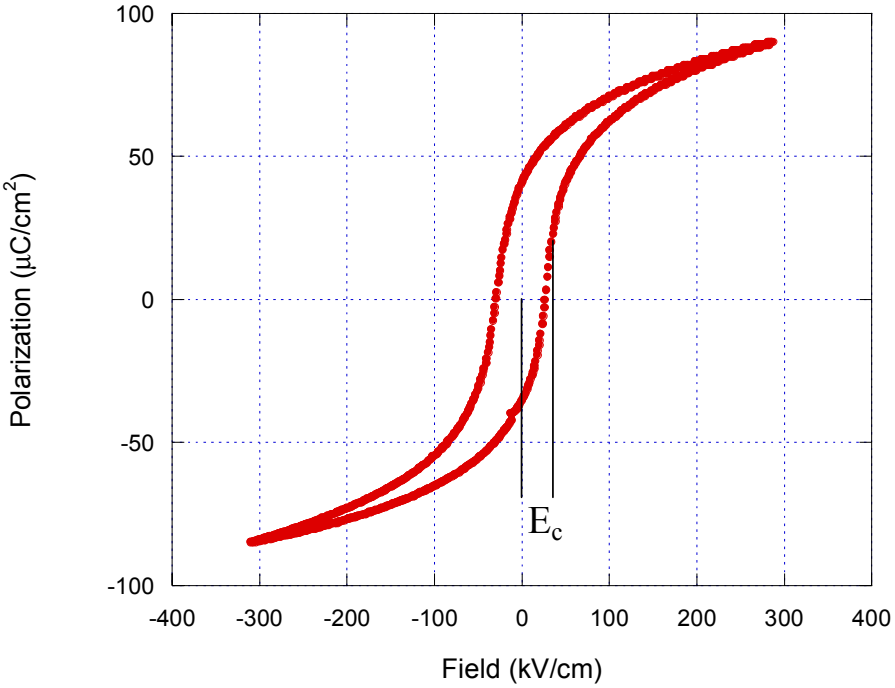

Figure 6.2. Polarization hysteresis loop for a 1 μm thick PZT film.

Samples were poled at roughly three times their coercive field (120 kV/cm) for ten minutes. The hysteresis curve, shown in figure 6.2, was measured using a Radiant Technologies RT 66A ferroelectric tester and the coercive field was obtained. It is important to measure the effect of time after poling when establishing a standardized test. The piezoelectric coefficients decay logarithmically with time, so if the material's properties are measured too quickly after poling the values will seem artificially high. Figure 6.3 shows the measured e_{31} value as a function of time after poling. It can be seen that the values decay logarithmically and level off around 24 hours after poling. From figure 6.3, it was determined that the tests should be performed at least 24 hours after the sample has been poled. This is within the range of logarithmic decrement that the values do not significantly change.

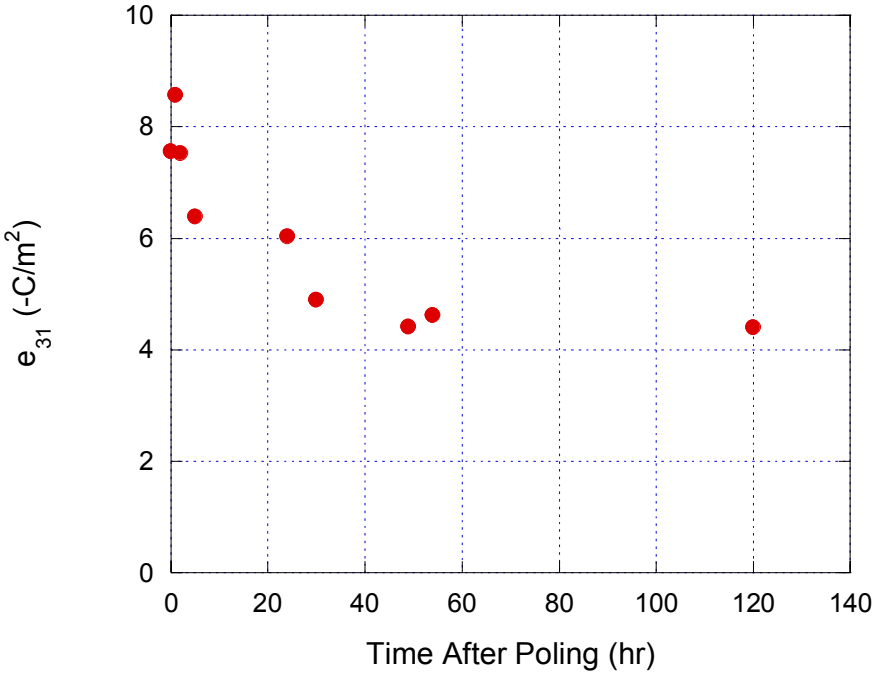

Figure 6.3. e_{31} as a function of time after poling for a 1 μm 40:60 conventionally annealed film poled at 120 kV/cm for 10 minutes. After 24 hours the value does not change significantly.

6.3 Composition

Two film compositions were investigated in this study, the morphotropic phase boundary composition of 52:48, and the tetragonal 40:60 composition. These films were prepared using the same solution deposition techniques as outlined in appendix A. Both films were 1 μm thick and poled under the same poling conditions, 120 kV/cm for 10 minutes and aged 24 hours before testing.

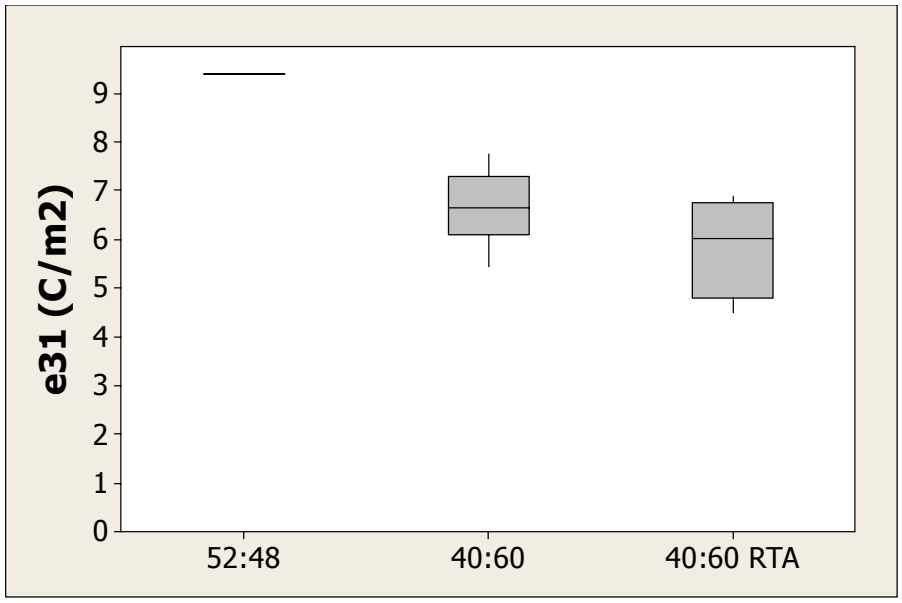

Figure 6.4. Boxplot comparing the e_{31} measurements for PZT films of varying composition and annealing conditions.

Using the RMM, an e_{31} value of –6.56 C/m^2 was measured for the 40:60 averaged from six films and a value of –9.4 C/m^2 was measured for 52:48 averaged from two films with two membranes tested from each film. The mean values including the standard deviation and the extents of the measurements can be seen in the boxplot in figure 6.4. From this plot it can be seen that the range of the 52:48 values is above the range of the 40:60 values with no overlap. These values are compared in figure 6.4, and it can be seen that there is a difference of 2.84 C/m^2, which indicates that the 52:48 films have significantly higher piezoelectric properties. However, from a device perspective it is important to also consider residual stress. From the pressure deflection data in figure 6.5 it can be seen that the 52:48 film is less compliant than the 40:60 film. For applications where residual stress is not a factor then the high piezoelectric properties of the 52:48 films are very attractive, but in the case of the P^3 generator the piezoelectric properties are only one of the many factors that affect device performance.

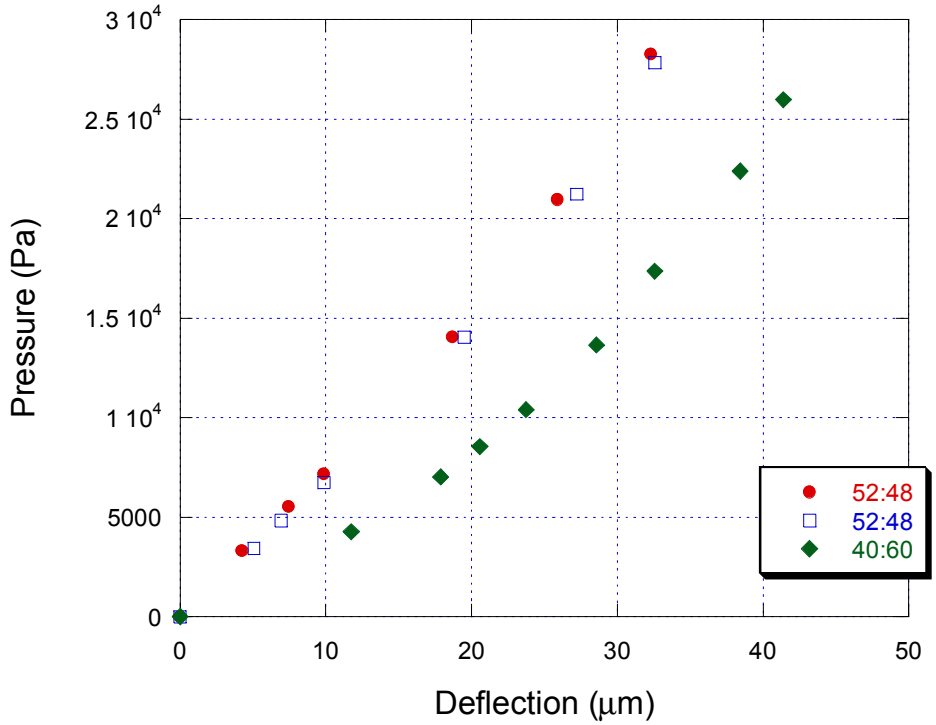

Figure 6.5. Pressure deflection curves for PZT films of varying composition.

6.4 Substrate Conditions

An important factor for the development of the RMM was to test the piezoelectric properties of the films used in the P^3 generator under the same processing and substrate conditions. Since the basis for the P^3 generator is the membrane structure the substrate condition effect on the properties is of interest. Methods such as the WFT and the cantilever method test the properties on solid substrates where the RMM tests film that are on membranes.

Differences between films on membranes and films on solid substrates could be attributed to differing thermal effects on membranes when pyrolyzing and annealing, the shape of the membrane when spinning on the PZT solution, or the compliance of the membrane when poling. It is common to observe color and clarity variations from the membranes to the rest of the wafer which could indicate variations in the film.

Using the cantilever method and the WFT, which use solid substrates, to compare values on membranes measured using the RMM the substrate condition can be evaluated. The piezoelectric properties of a 1 μm 40:60 PZT film annealed in the RTA measured using the cantilever method and the RMM were compared. A value of –4.38 C/m^2 (± 0.19 C/m^2) was measure using the cantilever method and a value of –5.06 C/m^2 (± 0.77 C/m^2) was measured using the RMM. Similarly, values measured using the WFT were compared with values measured using the RMM. For this comparison the same film could not be used, so two 1μm 40:60 PZT films conventionally annealed were compared. Using the WFT a value of –3.57 C/m^2 (± 0.26 C/m^2) was measured compared to –6.56 C/m^2 (± 0.74 C/m^2) for the RMM. Both situations show lower values for the films on solid substrates than on membranes. This indicates that the RMM is the ideal method for testing the films used in the P^3 generator because the values reflect the film conditions.

6.5 Summary of values

Piezoelectric properties of piezoelectric films have been measured using the wafer flexure technique, the cantilever method, conversion from field based measurements, and the rectangular membrane method. Results from these tests and other values found in the literature are compared in Table 6.1.

Material	Processing	Type of Test	Measurement device	Poling	Film Thickness [nm]	d31 [pC/N]	e31 [C/m^2]	Standard Dev. [C/m^2]	Number of Samples	Ref. #
PZT 45/55	2-butoxyethole Solution Deposition	Direct-cantilevers	Converse (input V meas. deflection		350	-12				50
PZT Composite	Acetic Acid Solution Deposition	Direct-normal load	HP 4263A Cap. Analyzer	220 kV/cm	750	124 calc. from g31 d31=$\varepsilon_0\varepsilon$g31				51
Bulk PZT	APC856 APC International	Converse-Frequency Analysis	HP 4192A impedance			-95				33
PZT 53/47	2-methoxyethanol Solution Deposition	Direct-cantilevers	Charge Amplifier	150 C, 250 kV/cm	880		**-6.83**			27
PZT 52/48	Solution Deposition	Direct-Wafer flexure technique	Charge integrating circuit	150 kV/cm		-59	**-8.66**			14
PZT 52/48	Solution Deposition	Converse-Clamped and Cantilevers	interferometric		500-2000	-33.9				49
PZT 52/48	APC841 APC International Machined Bulk	Direct-Strain-monitoring pneumatic	Strain gage TML FLA-1-11	300 kV/cm	1000	-60	**-7.89**			52
PZT 52/48	PZ26 Ferroperm Ltd.	Direct-conventional d_{33} meter		50 kV/cm for 5 min at 200 ^{0}C	10000		**-1.78**			31
PZT 54/46	Sputtered	Direct-cantilevers	Vmax using Oscilloscope	150 kV/cm			**-5.00**			16
PZT 40/60		Theoretical calculations	Theoretical calculations			-58.9				53
PZT 52/48	2-methoxyethanol Solution Deposition	Direct-cantilevers (WSU)	Charge integrating circuit	120 kV/cm for 1 min.	1000		**-7.12**	1.7	4	WSU
PZT 40/60	2-methoxyethanol Solution Deposition	Direct-cantilevers (WSU)	Charge integrating circuit	120 kV/cm for 1 min.	1000		**-5.85**	2.1	2	WSU
PZT 40/60	2-methoxyethanol Solution Deposition	Direct-cantilevers (WSU)	Charge integrating circuit	121 kV/cm for 10 min. aged 24 hr	1000	-43.4	**-4.38**	0.19	1	WSU
PZT 52/48	2-methoxyethanol Solution Deposition	Direct-Wafer flexure technique (WSU)	Charge integrating circuit	120 kV/cm for 10 min. aged 5 min	1000	-60.1	**-8.68**	0.56	1	WSU
PZT 40/60	2-methoxyethanol Solution Deposition	Direct-Wafer flexure technique (WSU)	Charge integrating circuit	120 kV/cm for 1 min. aged 5 min	1000	-38.6	**-5.57**	0.83	4	WSU
PZT 40/60	2-methoxyethanol Solution Deposition	Direct-Wafer flexure technique (WSU)	Charge integrating circuit	120 kV/cm for 10 min. aged 24 hr	1000	-24.7	**-3.57**	0.26	2	WSU
PZT 52/48	2-methoxyethanol Solution Deposition	Direct-Rectangular Membrane	Charge integrating circuit	120 kV/cm for 10 min. aged 24 hr	1000	-85.9	**-9.4**	1.5	4	WSU
PZT 40/60	2-methoxyethanol Solution Deposition	Direct-Rectangular Membrane	Charge integrating circuit	120 kV/cm for 10 min. aged 24 hr	1000	-60.2	**-6.56**	0.74	12	WSU
PZT 40/60 RTA	2-methoxyethanol Solution Deposition	Direct-Rectangular Membrane	Charge integrating circuit	121 kV/cm for 10 min. aged 24 hr	1000	-53.9	**-5.9**	1	4	WSU

Table 6.1. Piezoelectric properties found in literature and measured at WSU.

From this table it can be seen that the piezoelectric properties of the PZT films at WSU are very comparable to the values reported in the literature. It also shows that the values measured using the RMM correspond very well to values measured using other established methods.

CHAPTER SEVEN

COMPARISON OF e_{31} VERSUS e_{33} EFFECTS OF SPACING AND POLING

Through the use of the Rectangular membrane method, it was determined that the PZT synthesized at Washington State University and used in the P^3 generator is very comparable to PZT used by other researchers. It is necessary to understand the piezoelectric performance when looking at the device performance as a whole. If the PZT performance were below par it would reveal an area for improvement in device performance. Since the PZT performance is in fact good, other areas should be explored to improve device performance. Some of the major factors that affect this device performance are stress, environment, and structure. Structure is of particular interest and an alternative will be investigated, in this chapter.

One alternative electrode structure for use in the generator would incorporate interdigitated electrodes[60], which harvest charge in the 3-3 orientation. Typical e33 values are on the order of three times that of e_{31} [12,49]. The electrodes are patterned on the surface of the PZT as shown in figure 7.1. The "fingers" are alternately connected to the positive and negative electrode. When the material is poled the electric field penetrates the piezoelectric and orients the dipoles as shown in figure 7.2. 5, 10, and 15 micron spacing with 10 micron lines were used in this study. Holding to conventional poling practices, the samples were poled at a field of 120 kV/cm which corresponds to 120 V for 10 μm spacing compared to the 12 V for the 1 μm thick film on a conventional generator. At voltages as large as the ones used dielectric breakdown becomes an important consideration. If the samples are poled in air, dielectric breakdown will occur

and the electrode structure will be damaged. To prevent this the samples were poled in mineral oil.

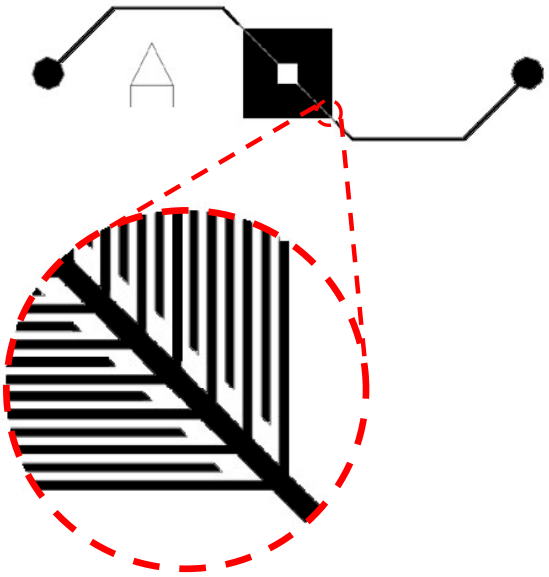

Figure 7.1. Interdigitated electrode structure for a 3 X 3 mm generator. The electrodes are 10 μm with 10 μm spacing.

Interdigitated electrodes are electrodes oriented on the surface of the piezoelectric so that the field is oriented in the 33 direction. This can best be shown by figure 6.2. With thin piezoelectric films the field will penetrate down into the film and the dipoles orient along the 3 axis. Therefore, when the piezoelectric is stressed the dipoles will alternate and a surface charge will be produced on the electrodes. Typically Pt or Ir is used as the substrate for PZT, because the orientation and grain size of these metals results in columnar, tetragonal PZT [61]. However, with this structure it is important that the piezoelectric is mounted on an insulating layer, to prevent the dipoles from aligning along the 1 axis. While this may complicate achieving optimal piezoelectric properties from PZT it is required due to the possibility of charge leakage.

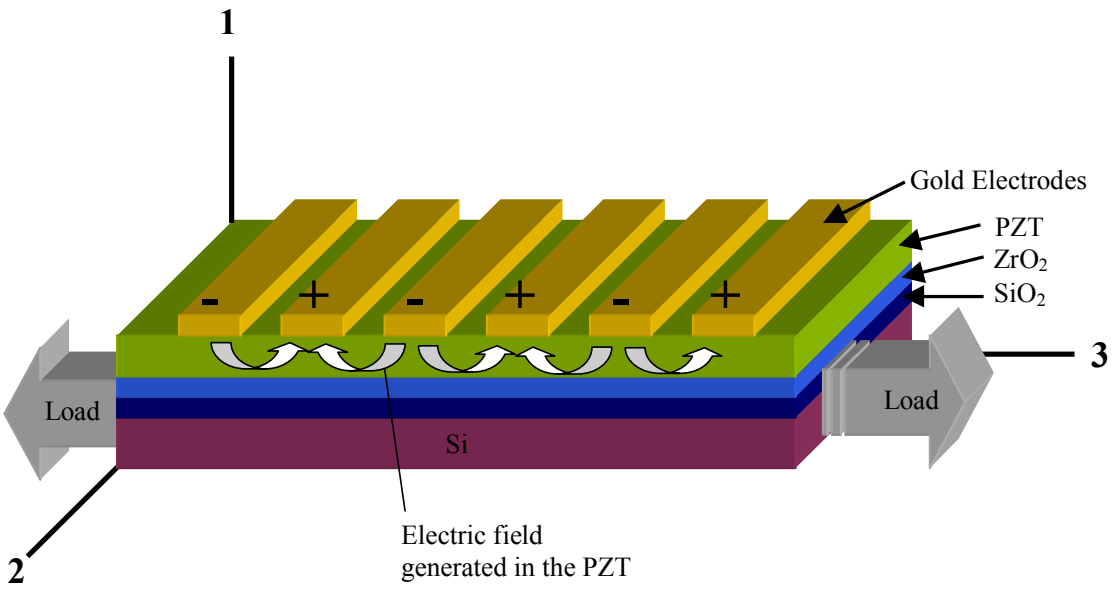

Figure 7.2. When a transverse stress is applied to the membrane a field is generated in the 3 direction.

For this study ZrO_2 was used as the insulation and barrier layer. It was deposited using a solution deposition process [60] similar to that used for the PZT, based on acetic acid (C_2OOH_4) as the solvent. A 0.35 molar solution was used, and 5 layers were deposited to achieve a film thickness of 140 nm. The PZT was solution-deposited as described in appendix A. An electrode was sputtered on top of the PZT consisting of a 5 nm TiW adhesion layer and then a 300 nm Au layer. The top electrode was patterned using contact photolithography with a chrome on glass mask to achieve the desired feature size. A cross section of the device can be seen in figure 7.3. The electrode spacing used in this study was limited by the contact lithography and the subsequent wet etching. Spacing will be discussed further in the following sections.

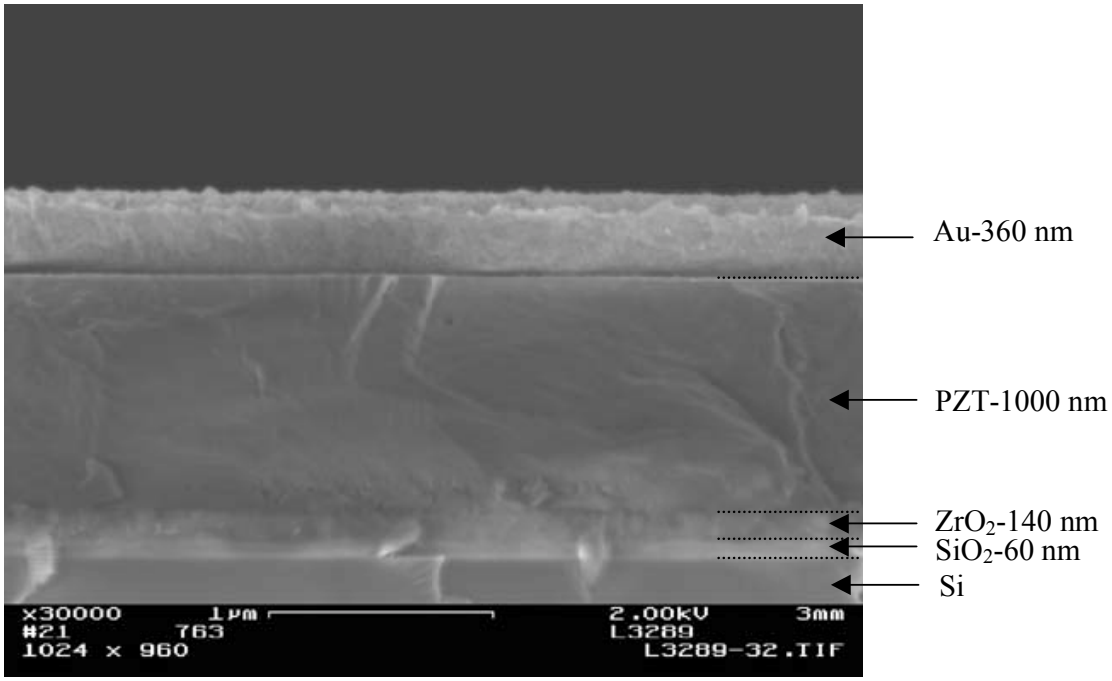

Figure 7.3. SEM cross section of IDE generator (courtesy of J. Martinez)

Samples prepared using this method did not perform better than samples having the conventional 3-1 orientation. The output was very low and residual stress was high due to the additional solution-deposited ZrO_2. The samples were tested on a RT66A ferroelectric tester. The hysteresis curves were not very distinct and did not show much ferroelectric behavior, this can be seen in figure 7.4. Depositing the PZT on ZrO_2 leads to differences in the film from those deposited on platinum. The standard 3-1 oriented structure with a platinum bottom electrode has been researched and optimized for several years. Depositing the PZT on ZrO_2 was not optimized for this substrate but the same deposition technique as used for a 3-1 structure was used which did not result in the best possible films.

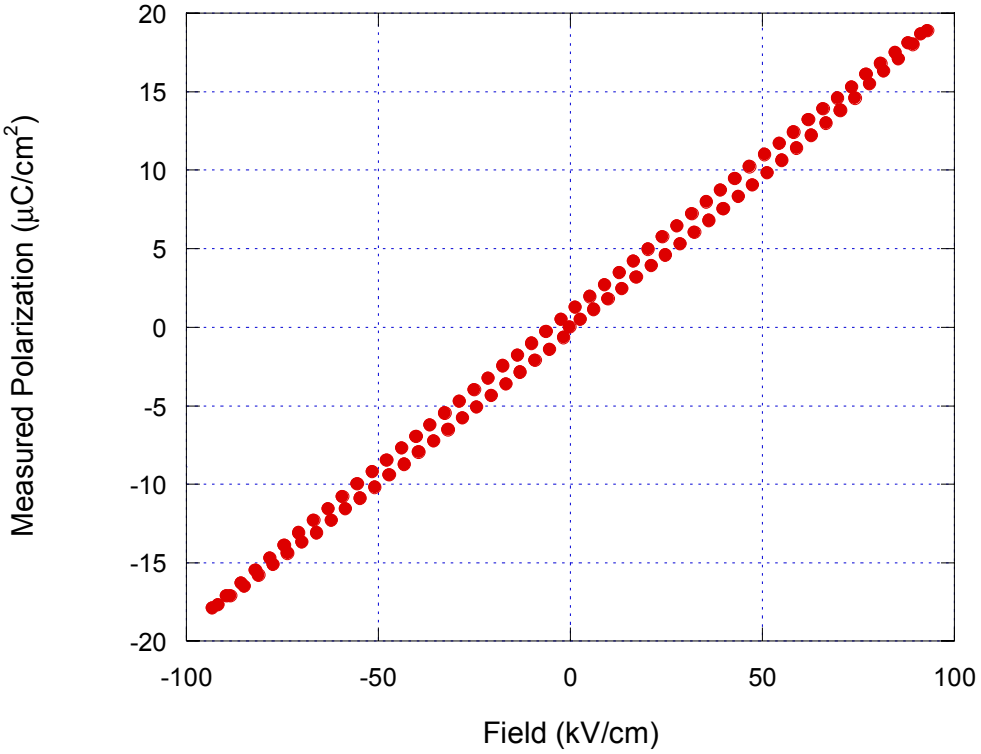

Figure 7.4. Ferroelectric hysteresis plot for IDE rectangular structure with 10 μm lines and 10 μm spacing.

IDE samples were tested using the RMM, as described in section 5.1, to get the charge given off for a given strain. The charge produced on a IDE rectangular electrode structure, with 75 –10 μm lines spaced 10 μm apart, was one order of magnitude lower than that for a conventional RMM sample with a .5 X 3 mm electrode. This experimental data was fit to the pressure deflection relation

$$P = \frac{E}{1-\nu}\frac{t^3 h}{a^4}\left[\frac{1}{12\alpha(1+\nu)} + C\frac{h^2}{t^2}\right] + C^*\frac{\sigma_0 th}{a^2} \tag{41}$$

where α, C, and C* are geometric parameters with values of $2.6\text{x}10^{-3}$, 9.82, and 6.47 for 2 X 8 mm membranes [45]. By fitting this pressure deflection relation the residual stress

and composite modulus values were found, which were determined to be 100 MPa and 125 GPa, respectively.

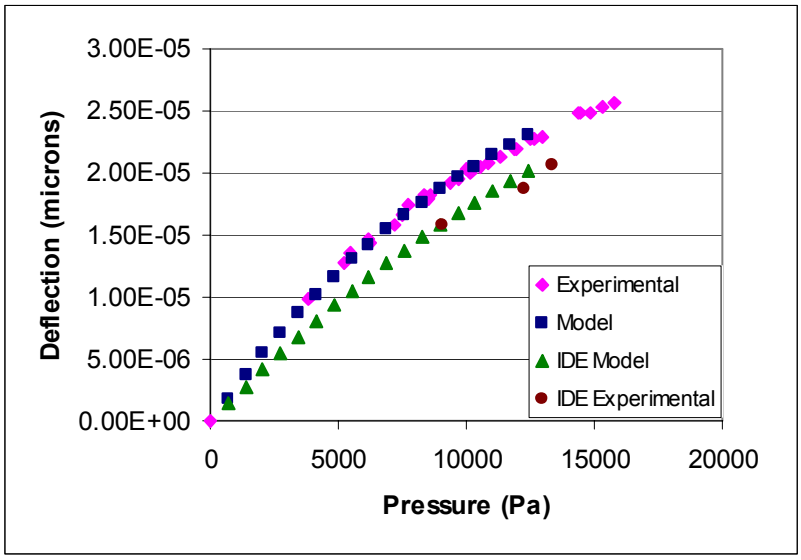

Figure 7.5. Pressure deflection for the conventional and for IDE samples.

Since the experimental and calculated pressure deflection matched up well, the next step was to match the charge produced for a given strain to find the d_{33} value of the PZT used for the IDE structure. The charge was measured experimentally for a given pressure which was used to calculate the PZT stress as

$$\sigma_{PZT} = \frac{2}{3}\frac{h_0^2}{a^2}\frac{E_{PZT}}{(1-\nu^2)} \tag{42}$$

where a PZT modulus of 115 GPa and a Poissons ratio of 0.27 were used. Calculating the stress in the PZT from the deflection calculations it was determined that the IDE d_{33} value was equal to 30 pC/N. The calculated charge is compared to the charge measured experimentally in figure 7.6. It can be seen that the calculated values are very similar to the experimental values, suggesting our value of d_{33} = 30 pC/N is appropriate.

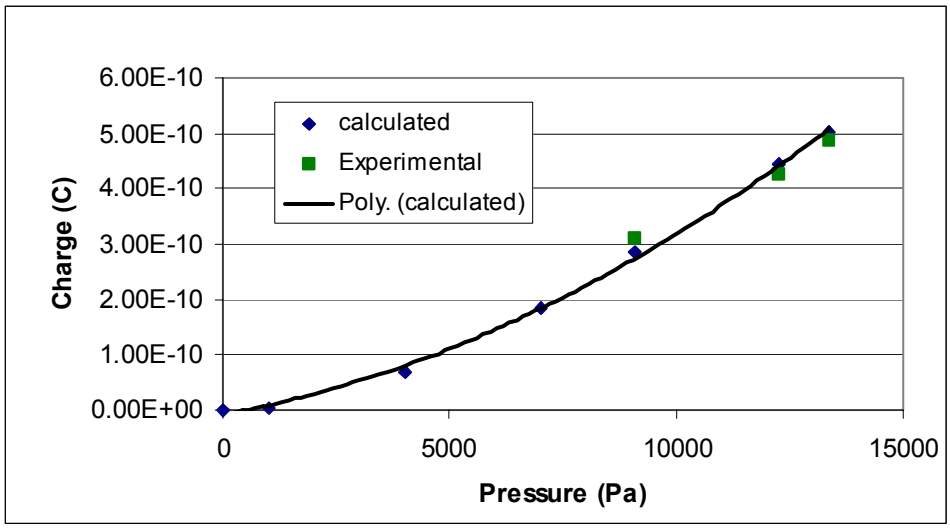

Figure 7.6. The calculated charge is compared to the experimentally measured charge to find d_{33}.

Model parameters were further adjusted to see if the interdigitated electrodes could compare with the conventional electrode structure. The electrode area and the d_{33} values are used to calculate the amount of charge that will be collected for a given stress, which is calculated using equation 42. From figure 7.7 it can be seen that the interdigitated electrodes could potentially produce almost twice the charge of a conventional structure. However, the properties necessary to achieve this output are not feasible. The model is based off 2 micron interdigitated electrodes with 0.25 micron spacing between them and 2.75 micron thick PZT with a d_{33} value of 200 pC/N. In figure 7.7 it can be seen that these parameters were the optimal conditions for the IDE structure.

Longitudinal piezoelectric coefficients are typically two or three times the transverse piezoelectric coefficients. A d_{33} value of 200 pC/N is a high estimate but is similar to values reported in literature for thin PZT films of similar composition [11,32,52,62,63]. Bulk d_{33} values for similar PZT are typically about 215 pC/N, which is a upper bound for thin films since thin film values are normally lower than bulk [64].

Values as high as 180 pC/N were reported for thin films measured using a pneumatic pressure rig [52]. More typical values measured using a pneumatic pressure rig are around 100 pC/N [62]. The use of 200 pC/N for the model is high but acceptable in representing the highly idealized parameters.

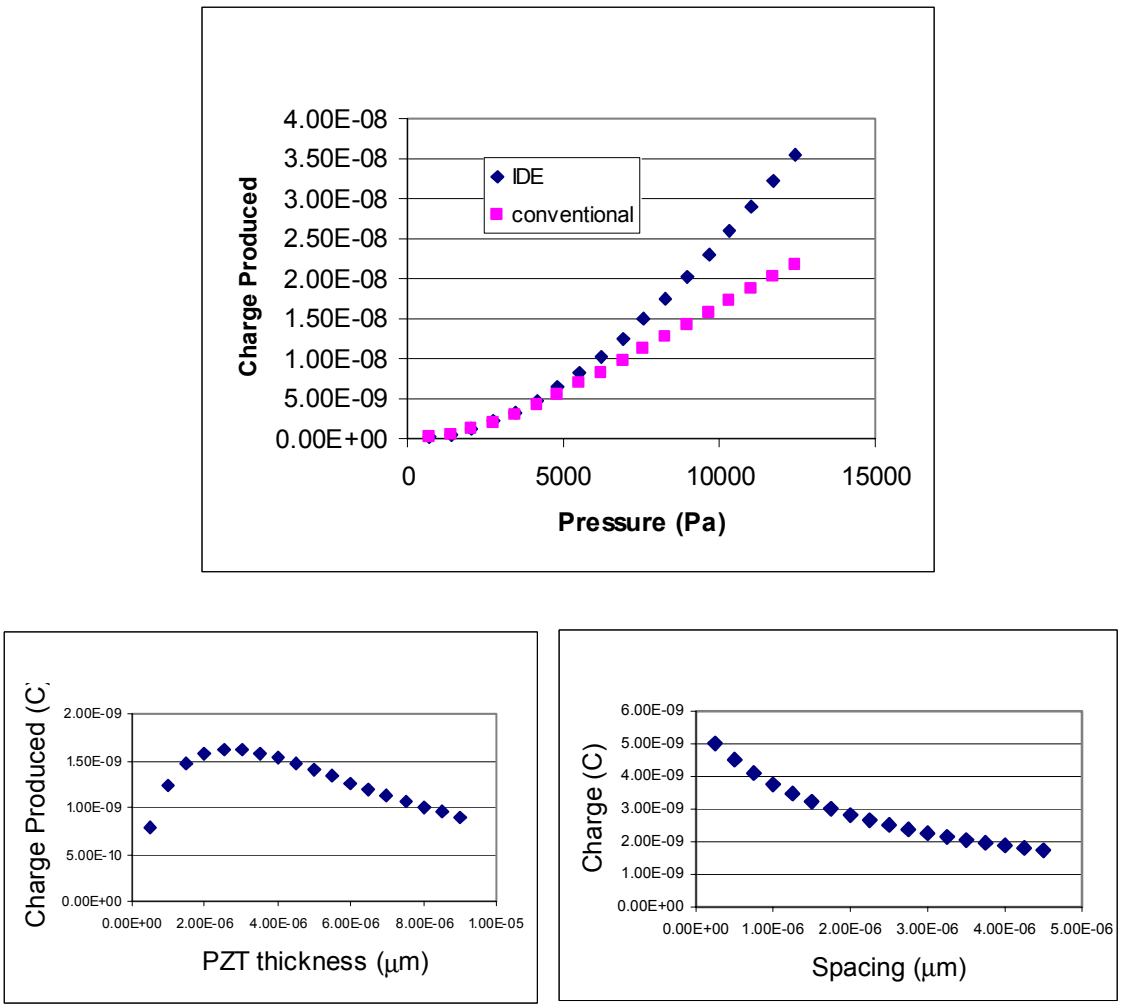

Figure 7.7. Top: Charge output from model comparing optimized rectangular IDE structure to conventional RMM structure. Bottom: The PZT thickness and the electrode spacing were varied using the model to determine the optimal parameters.

The initial problem is the electrode adhesion would have to be very good in order to get 2 micron lines to stay on the PZT. Spacing below 5 microns is difficult to achieve.

Using contact lithography and the chrome on glass mask, it was difficult to etch the photoresist the correct time to eliminate all bridging but not to undercut and change the line widths. In addition, the electrodes would often bridge the electrodes, creating shorts between the electrodes.

From this study it can be determined that interdigitated electrodes are not the path that should be further explored in attempting to reach the goal of improving generator performance. In order to compare with a non-optimized conventional structure the fabrication would involve fabrication that is only done at the most state-of-the-art development facilities. Some of the same problems still exist with the IDE structures, for instance the large residual stresses that result from solution deposited PZT films.

CHAPTER EIGHT

CONCLUSIONS AND FUTURE WORK

Piezoelectric properties in the form of the universally accepted d_{31} and e_{31} have been measured using the Rectangular Membrane Method. This method was validated using other methods commonly used in literature. The cantilever method was used, which uses the center portion of the wafers used to perform the RMM. This ensures that the film composition and deposition method are the same. The wafer flexure technique was used to determine the piezoelectric coefficients of the films fabricated at WSU. However this method uses individual test structures so films of the same composition and processing on different wafers were compared. In addition a method for converting from strain-based measurements, previously developed at WSU, to e_{31} was established and verified. The RMM was used in studies to determine the affect of conventional versus rapid thermal annealing, the affect of the PZT film composition, and the substrate condition on the piezoelectric properties. The standard poling procedure was also investigated to ensure that the values measured were truly representative of the device properties. An alternate generator structure was developed and tested to determine if it could increase performance.

The RMM was developed as a method of measuring the transverse piezoelectric properties of the PZT film used in the P^3 generator. Test devices were designed so that the RMM test die could be fabricated in parallel on the same wafer as the P^3 generator. This enabled a true measurement of the piezoelectric properties as they exist in the P^3 generator. In addition it provided a way to convert from the specific voltage measurements previously used to evaluate the piezoelectric films. This is useful because

it provides a way to compare films used in the past with the films used today. The values obtained by converting from the specific voltage provide a low-end estimate that is 80% of the measured value.

It was found that typical values for solution-deposited PZT thin films synthesized at WSU and annealed in a conventional furnace with a titanium to zirconium ratio of 40:60 are an e_{31} of –6.56 C/m^2 and a d_{31} of –76.0 pC/N. These values are for 1 μm thick films poled at 120 kV/cm and aged for 24 hours. The d_{31} value is for a measured PZT Young's modulus of 80 GPa [38]. This is compared with PZT films of 40:60 composition annealed in the RTA. The e_{31} value measured for this film is –4.63 C/m^2. In addition films with he morphotropic phase boundary composition, 52:48, were tested and values of –9.4 C/m^2 and –108.5 pC/N, using the measured 80 GPa Young's modulus, were typical.

From the values measured using the RMM it can be concluded that PZT films with 52:48 composition have the highest piezoelectric properties followed by the conventionally annealed 40:60 films and then the 40:60 RTA annealed films. For use in the P^3 generator evaluating the piezoelectric properties alone is not sufficient. The 52:48 film is much less compliant than the 40:60 film and similarly the RTA film is less compliant than the conventionally annealed films. The optimization of the piezoelectric parameters with the films mechanical properties should be investigated.

Comparing films on solid substrates using the cantilever method to films on membranes using the RMM it is evident that the films on the solid substrate have lower piezoelectric properties. The heating rates and the stress conditions can very from solid

substrates to membranes. These variations can lead to the differences in the piezoelectric properties.

Time after poling was also investigated to see if it had a significant affect on properties. It was observed that the piezoelectric properties decay logarithmically with time after poling. The rate of decay is very small after 24 hours. Therefore it was determined that the RMM should be performed at least 24 hours after poling. This guideline makes it possible to compare values from films tested 24 hours after poling with films that were poled days earlier, and only experience minimal decline in values.

Through the use of the RMM it was determined that the PZT synthesized at WSU exhibits good piezoelectric properties. The values measured are very comparable to values reported by other researchers. So in order to increase device performance other structures were investigated that utilize the longitudinal piezoelectric properties which are normally three time larger than the transverse properties. The interdigitated electrode structure investigated did not improve device performance. The properties that were desired could not be realized using the fabrication techniques and tools at WSU. In addition the fabrication steps required to from the interdigitated structure significantly lowered compliance, which reduces the generator performance. Other, more promising, structures to enhance generator performance are being investigated and future development should continue to explore ways to best take advantage of the high piezoelectric properties of PZT and reduce the high stress.

APPENDIX A

FABRICATION PROCEEDURES

e_{31} Wafer Fabrication

1. Begin with 3" (100) silicon wafer with boron diffused on one side and with a low temperature oxide grow on both sides.
2. Pattern the backside of the wafer using the e_{31} wafer mask and etch the oxide using BOE. Remove the photoresist and place the wafer in EDP etchant for 6 hours to etch the pits.
   Bottom Electrode
3. Clean the wafer using the five step process (Acetone, IPA, DI rinse, Acetone IPA) and blow dry using canned air.
4. Load the wafer boron side up on the rotary sample holder. Securely fasten using the screws. Vent the sputtering chamber and wait until it displays SEALED.
5. Open the chamber and load the targets, Ti on the back gun and Pt on the front gun.
6. Load the rotary sample holder and shut the door.
7. Press the CYCLE button and pump down for at least 12 hours or a pressure of $8X10^{-7}$ torr.
8. Sputter the Ti and then the Pt and remove wafer from the chamber.
9. Anneal the Pt in the conventional furnace at 650 ^{0}C for 10 minutes before spinning PZT.
10. Spin PZT following the standard procedures.
11. Load Au and TiW targets into the sputtering chamber. TiW on the back gun and Au on the front.
12. Load the wafer on the rotary work holder.
13. Load the rotary work holder and shut the chamber door.
14. Press the CYCLE button and let pump down to a pressure of $8X10^{-7}$.
15. Sputter the TiW and Au.
16. Remove the wafer and pattern using the e_{31} top electrode mask and the standard photolithography procedure.
17. Etch the exposed gold using gold etchant type TFA.
18. clean using five step process (Acetone, IPA, DI rinse, Acetone IPA)
19. Pattern the wafer using the PZT etch mask.
20. Etch the exposed PZT using the PZT etchant.
21. clean using five step process (Acetone, IPA, DI rinse, Acetone IPA)
22. Wafer is ready for testing.

Rapid Thermal Annealing (RTA) Procedures

1. DO NOT operate this equipment if you have not been cleared by the Lab Manager.
2. Check main cooling water. Turn Cold water valve at fume hood two turns on.
3. Check Pyrometer cooler
    a. Power ON
    b. Press UP or DOWN buttons to set temperature to 17.0C
    c. Press ENTER on cooler
    d. Press START on cooler, There should be a "-" symbol on the left hand side of the LCD display. DO NOT run RTA until temperature stabilizes at 17.0C.
4. Verify that RTA mains power is ON
5. Make sure that the RTA "TEMP MON" switch is set to T.C.
6. Make sure that the RTA "LAMP CONTROL" switch is set to AUTO.
7. Make sure that the RTA "EMISSIVITY" thumbwheel is set to 50.
8. Verify that the compressed air regulator is set to 20 PSI
9. Verify that the N_2 supply valve is ON
10. Turn on the RTA front panel power switch.
11. Verify that the green power indicator light is ON.
12. Start the "HEATPULSE 610" software, click on the "RTP Control Pages" button. Then click on the "Run Process" button.
13. Verify that the "Over Temp Setpoint" is set to 1200.
14. Set the "Purge MFC set point, SLM" to 0.0
15. DO NOT turn on the "Adaptive Learn" button.
16. Perform a test run for your recipe with the Dummy wafer to verify proper operation.
17. A wafer MUST be in the chamber, on the holder or in a suseptor, during any run. Failure to do so will damage the RTA.
18. Verify that there is a Dummy wafer in the furnace. Get the Dummy wafer from the wafer box if the furnace is empty.
19. Make sure the Dummy wafer is loaded polished side down and centered on the holder. If using a suseptor, the dummy wafer is still polished side down, and the lid is placed over it.
20. Slowly and gently, close and lock the furnace door. Quick moves will drop the wafer in the furnace.
21. Select the appropriate Pyrometer Calibration file. They will be named "Si_wafer_calxx" or "SiC_suseptorxx".
22. Select the “700_30sec_pyr.txt” recipe.
23. Press and hold the "Start" button for 2-3 seconds. Verify that the program continues to run after the button is released.
24. Watch the program run, Wait for it to end. Do not step away while the system is heating. If the system runs much hotter than intended or does not stop at the appropriate time, press the stop button. If there is still a problem, turn off the RTA front panel power switch and notify the lab manager.
25. When the run ends, wait for the "Control Temperature" to drop below 30C to allow the quartzware and wafer to cool to handling temperature.

26. Open the furnace drawer slowly and gently. If the quartzware, wafer, or suseptor is still radiating heat, close drawer and wait for it to cool further.
27. Remove the dummy wafer and place it in the wafer box after verifying that it is cool. DO NOT place the wafer on any surface. It will pick up contamination that will be transferred to the RTA. Do not place the suseptor on any surface other than in its container.
28. If the recipe runs as expected, repeat the steps 20-24 with your own wafers. Place your wafer PZT side UP. If your wafer has membranes, take care to not pierce them with the support points if not using suseptor. If you are running a different recipe, repeat the first run with a dummy wafer.
29. When cool, remove suseptor and place it on a clean wiper. Place another wiper on top and turn over the whole stack. Remove the top towel and suseptor base and remove your wafer from the lid with wafer tweezers.
30. When finished with the run, replace the dummy wafer in the chamber, polished side down.
31. Wait at least 10 minutes after the last run before you Shut down the RTA.

To shut down:

32. Exit the Heatpulse 610 software.
33. Turn off the N_2 supply
34. Turn off the front Heatpulse 610 front panel power switch.
35. Turn off the Pyrometer Cooler power.
36. Leave on the Main Power Fusebox.
37. Leave on the cooling water at fumehood.
38. Leave the compressed air supply at 20 PSI

ZrO_2 Solution Synthesis

1. Warm up the hotplate with the mineral oil bath on it, set it to 4.4 (105 ^{0}C), at least 1 hour before preparing solution.
2. Remove 250 ml two-neck flask, reflux tower, hose fittings, and flask stoppers from the oven. Allow to cool for 30 minutes.
3. Put a stir bar in the flask. Place two-neck flask into the load lock.
4. Pull a 12 psi vacuum in the load lock and then purge with nitrogen. Repeat three times.
5. Load the flask into the glove box. Measure out the proper amount of acetic acid solution from table A.1, and add to the flask.
6. Measure out the proper amount of Zirconium n-propoxide and add to the acetic acid in the flask.
7. Put the stoppers in the flask and remove from the glove box.
8. Place the flask in the stand and set up the equipment as shown in figure A.1.
9. Reflux at 105 ^{0}C for 1 hour. Add distilled water and ethylene glycol during reflux to the solution if precipitate forms.
10. Lower oil bath and allow to cool for 20 minutes.
11. Place the flask and a glass storage container in the load lock and purge three times.
12. Pour solution and stir bar into the storage container.
13. Remove flask and clean in the fume hood using acetone. Pour into waste container. Place rinsed glassware into a large nalgene container filled with DI water.
14. Rinse at the sink with DI water and place in the oven to dry.

Molarity	Mass Zr for 1 mL solution (g)	Vol of Zr for 1 mL of Solution (mL)	Vol of C2H4O2 for 1 mL of Solution (mL)	Mass of C2H4O2 for 1 mL of Solution (g)
1	0.468	0.448	0.552	0.579
0.95	0.445	0.426	0.574	0.603
0.9	0.421	0.403	0.597	0.626
0.85	0.398	0.381	0.619	0.650
0.8	0.374	0.359	0.641	0.673
0.75	0.351	0.336	0.664	0.697
0.7	0.328	0.314	0.686	0.721
0.65	0.304	0.291	0.709	0.744
0.6	0.281	0.269	0.731	0.768
0.55	0.257	0.247	0.753	0.791
0.5	0.234	0.224	0.776	0.815
0.45	0.211	0.202	0.798	0.838
0.4	0.187	0.179	0.821	0.862
0.35	0.164	0.157	0.843	0.885
0.3	0.140	0.134	0.866	0.909
0.25	0.117	0.112	0.888	0.932
0.2	0.094	0.090	0.910	0.956
0.15	0.070	0.067	0.933	0.979
0.1	0.047	0.045	0.955	1.003
0.05	0.023	0.022	0.978	1.026
0	0.000	0.000	1.000	1.050

	20 mL Batch	
Molarity	Mass Zr (g)	Mass C2H4O2 (g)
1	9.359	11.587
0.95	8.891	12.057
0.9	8.423	12.528
0.85	7.956	12.999
0.8	7.488	13.469
0.75	7.020	13.940
0.7	6.552	14.411
0.65	6.084	14.881
0.6	5.616	15.352
0.55	5.148	15.823
0.5	4.680	16.293
0.45	4.212	16.764
0.4	3.744	17.235
0.35	3.276	17.705
0.3	2.808	18.176
0.25	2.340	18.647
0.2	1.872	19.117
0.15	1.404	19.588
0.1	0.936	20.059
0.05	0.468	20.529
0	0.000	21.000

	40 mL Batch	
Molarity	Mass Zr (g)	Mass C2H4O2 (g)
1	18.719	23.174
0.95	17.783	24.115
0.9	16.847	25.056
0.85	15.911	25.998
0.8	14.975	26.939
0.75	14.039	27.880
0.7	13.103	28.821
0.65	12.167	29.763
0.6	11.231	30.704
0.55	10.295	31.645
0.5	9.359	32.587
0.45	8.423	33.528
0.4	7.488	34.469
0.35	6.552	35.411
0.3	5.616	36.352
0.25	4.680	37.293
0.2	3.744	38.235
0.15	2.808	39.176
0.1	1.872	40.117
0.05	0.936	41.059
0	0.000	42.000

Table A.1. Quantities for making ZrO_2 solution.

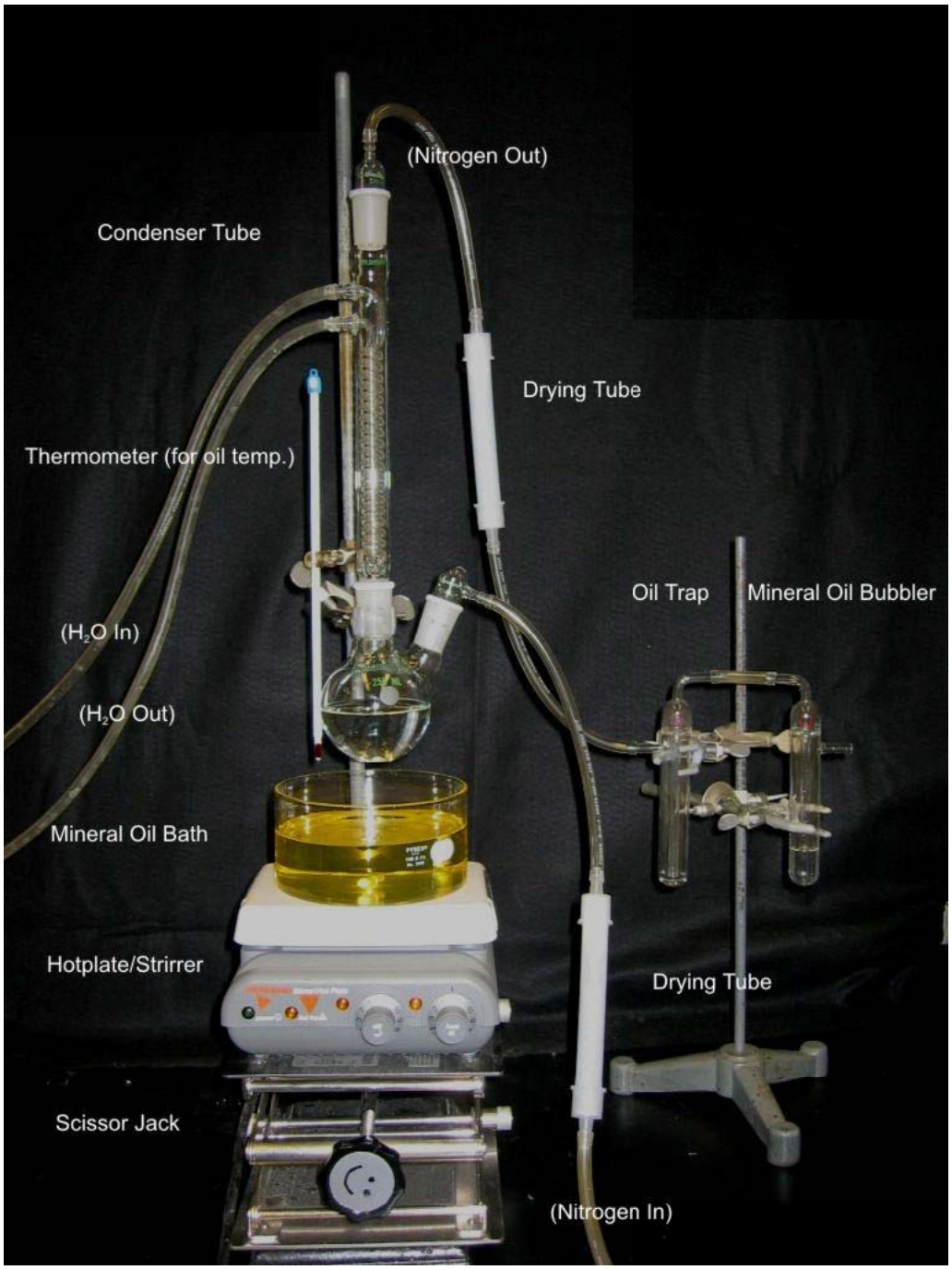

Figure A.1. Reflux set up.[23]

ZrO_2 Solution Deposition

1. Load 5 cc syringe into load lock
2. Pull a 12 psi vacuum in the load lock and purge with nitrogen. Repeat three times.
3. Fill with solution and remove from glovebox.
4. Go to the cleanroom and turn the conventional annealing furnace to 600 ^{0}C.
5. Gown up and enter the cleanroom
6. Turn on the hotplate to 420 ^{0}C and allow to heat up until the thermocouple reads 375 ^{0}C (this will probably correspond to the hotplate set at 420 ^{0}C).
7. Center the wafer on the spincoater chuck and verify that it is set to spin at 3000 rpm for 30 seconds.
8. Deposit solution on the wafer from the outside working inward.
9. Press the START button and allow to spin.
10. When wafer stops press the RESET button and flip the VACUUM switch.
11. Pyrolyze at 375 ^{0}C for 2 minutes.
12. Anneal in the conventional furnace at 600 ^{0}C for 6 minutes.
13. After five layers anneal at 700 ^{0}C for 3 hours in the conventional furnace.
14. The film is ready for PZT deposition.

References:

1. http://www.aero.org/publications/aeropress/Helvajian/Helvajian_1_1.html
2. A. Frazier, R. Warrington, C. Friedrich, "Miniaturization Technologies: Past, Present, and Future". IEEE Transactions on Industrial Electronics Vol. 42 (2), 1995 423-430
3. J. Curie and P. Curie, Bull. Soc. Mineral. De France 3, 90-93 (1880).
4. S. Whalen, M. Thompson, D.F. Bahr, C.D. Richards, R.F. Richards. "Design, Fabrication, and Testing of the P^3 Micro Heat Engine", Sensors and Actuators A 104 (2003) 290-298
5. Aireus Christensen. *Fabrication and characterization of a liquid-metal micro-droplet thermal switch*. Masters Thesis, Washington State University. August 2003.
6. Robert Gifford, *Resonant Frequency Characterization of a Novel MEMS Based Membrane Engine.* Masters Thesis, Washington State University. June 2004.
7. W.D. Callister, Jr. Materials Science and Engineering an Introduction, John Wiley and Sons, Inc. p. 388, 648-649 (2000)
8. D.L. Polla, L.F. Francis, "Processing and Characterization of Piezoelectric Materials and Integration into Microelectromechanical Systems", Annu. Rev. Mater. Sci. 1998. 28:563-97
9. J.G. Smits, W. Choi, "The Constituent Equations of Piezoelectric Heterogeneous Bimorphs". IEEE Transactions on Ultrasonics, Ferroelectrics, and Frequency Control. Vol. 38, NO. 3, May 1991 256-270
10. IEEE Standard, 176-1987
11. J.-M. Liu, B. Pan, HL.W. Chan, S.N. Zhu, Y.Y. Zhu, Z.G. Liu, "Piezoelectric Coefficient Measurement of Piezoelectric Thin Films: an Overview". Materials Chemistry and Physics 75 (2002) 12-18
12. P. Verardi, F. Craciun, M. Dinescu, "Characterization of PZT Thin Film Transducers Obtained by Pulsed Laser Deposition". IEEE Ultrasonics Symposium (1997) 569-572
13. K. Lefki, G. Dormans, "Measurement of Piezoelectric Coefficients of Ferroelectric Thin Films". Journal of Applied Physics 76 (3), 1994 1764-1767
14. J.F. Shepard Jr., P.J. Moses, S. Trolier-McKinstry, "The Wafer Flexure Technique for the determination of the Transverse Piezoelectric Coefficient (d31) of ZT Thin Films". Sensors and Actuators A 71 (1998) 133-138
15. J.F. Shepard Jr, F. Chu, I. Kanno, S. Trolier-McKinstry, "Characterization and Aging Response of the d31 Piezoelectric Coefficient of Lead Zirconate Titanate Thin Films". Journal of Applied Physics 85 (9), 1999 6711-6716
16. E. Cattan, T. Haccart, and D. Remiens, "e_{31} Piezoelectric Constant Measurement of Lead Zirconate Titanate Thin Films". Journal of Applied Physics 86 (12), 1999 7017-7023
17. I. Kanno, S. Fujii, T. Kamada, and R. Takayama, "Piezoelectric Properties of c-axis Oriented Pb(Zr,Ti)O3 Thin Films". Applied Physics Letters 70 (11), 1997 1378-1380

18. L.M.R. Eakins, B.W. Olson, C.D. Richards, RF. Richards, and D.F. Bahr, "Influence of Structure and Chemistry on Piezoelectric Properties of Lead Zirconate Titanate in a Microelectromechanical Systems Power Generation Application". Journal of Materials Research 18 (9), 2003 2079-2086
19. W. G. Cady, "Piezoelectricity", (original edition 1946, McGraw –Hill, New York, NY), revised edition, Dover Publications, New York, NY, 1964
20. J. Bernstein, et. al., "Micromachined Ferroelectric Transducers for Acoustic Imaging". Preceding of Transducers'97, The 1997 International Conference on Solid-State Sensors and Actuators, Chicago, IL, June 16-19, 1997, vol. 1, pp 421-424
21. J.W. Gardner, "Microsensors: Principals and Applications". John Wiley and Sons, New York, NY 1994
22. Gregory T.A. Kovacs, Micromachined Transducers Sourcebook McGraw Hill, Boston, pp. 33-39 (1998).
23. Bennet Olson , *Optimization of a Piezoelectric Membrane Generator*. Masters Thesis, Washington State University, August 2002.
24. Adam Olson, *Processing and Properties of a Piezoelectric Membrane Generator*. Masters Thesis, Washington State University, May 2003.
25. Jack Skinner, *Piezoelectric Membrane Generator Characterization and optimization*, Masters Thesis, Washington State University, December 2002.
26. S.P. Timoshenko, J.N. Goodier, Theory of Elasticity, Third edition, McGraw-Hill, Kogakusha, Tokyo,1970
27. M.A. Dubois, P. Muralt, "Measurement of the Effective Transverse Piezoelectric Coefficient $e_{31,f}$ of AlN and $Pb(Zr_x,Ti_{1-x})O_3$ Thin Films". Sensors and Actuators 77 (1999) 106-112.
28. V. Ziebart, O. Paul, U. Munch, J. Schwizer, H. Baltes, "Mechanical Properties of Thin Films from the Load Deflection of Long Clamped Plates". Journal of Microelectromechanical Systems 7 (1998) 320-328
29. J.J. Vlassak, W.D Nix, "A New Bulge Test Technique for the Determination of Young's Modulus and Poisson's Ratio of Thin Films". J. Mater. Res., Vol. 7, No. 12, Dec 1992 3242-3249
30. Owen Crabtree. Modeled using Finite Difference Code
31. J.E. Southin, S.A. Wilson, D. Schmitt, R.W. Whatmore, "$e_{31,f}$ Determination for PZT Films Using a Conventional 'd33' Meter". Journal of Physics D: Applied Physics 34 (2001) 1456-1460
32. J. Erhart, L. Burianova, "What is Really Measured on a d33-meter". Journal of the European Ceramic Society 21 (2001) 1413-1415
33. L. Burianova, M. Sulc, M. Prokopova, "Determination of the Piezoelectric Coefficients dij of PZT Ceramics and Composites by Laser Interferometry". Journal of the European Ceramic Society 21 (2001) 1387-1390
34. Q.M. Zhang, W.Y. Pan, and L.E. Cross, "Laser interferometer for the study of piezoelectric and electrostrictive strains". Journal of Applied Physics 63 (1988) 2492

35. P. Muralt, A. Kholkin, M. Kohli, T. Maeder, "Piezoelectric Actuation of PZT Thin-Film Diaphragms at Static and Resonant Conditions". Sensors and Actuators A 53 (1996) 398-404.
36. P. Luginbuhl, G.-A. Racine, P. Lerch, B. Romanowicz, K.G. Brooks, N.F. de Rooij, P. Renaud, N. Setter, "Piezoelectric Cantilever Beams Actuated by PZT sol-gel Thin Film". Sensors and Actuators A 54 (1996) 530-535
37. A. Ugural, Stresses in Plates and Shells, McGraw-Hill, 1981
38. Marian S. Kennedy, *Mechanical Property Determination of Thin Films for PZT MEMS Applications*. Masters Thesis, Washington State University 2003
39. W.W. Gerberich, W. Yu, D. Kramer, A. Strojny, D. Bahr, E. Lilleoden, and J. Nelson, "Elastic Loading and Elastoplastic Unloading from Nanometer Level Indentations for Modulus Determination". Journal of Materials Research, vol. 13, pp. 421-439 (1998)
40. A.L. Kholkin, Ch. Wutchrich, D.V. Taylor, and N. Setter, "Interferometric Measurements of Electric Field-Induced Displacements in Piezoelectric Thin Films". Review of Scientific Instruments 67 (1996) 1935-1941
41. A.J. Moulson, J.M. Herbert, Electroceramics, Chapmin & Hall, London, 1990
42. Micro Measurements, Bulletin 309E, pp. 17-26
43. http://www.piezo.com/intro.html
44. W.P. Mason, "Fifty Years of Ferroelectricity". The Journal of The Acoustical Society of America 50 (1971) 1281-1298
45. E. Bonnette, P. Delobelle, L. Bornier, B. Trolard, and G. Tribillon, "Two Interferometric Methods For the Mechanical Characterization of Thin Films by Bulging Tests. Application to Single Crystal of Silicon". Journal of Materials Research 12 (1997) 2234-2248
46. A.J. Kalkman, A.H. Verbruggen, G.C.A.M. Janssen, and F.H. Groen, "A Novel Bulge-Testing Setup for Rectangular Free-Standing Thin Films". Review of Scientific Instruments 70 (1999) 4026-4031
47. T. Tuchiya, T. Itoch, G. Sasaki, T. Suga, "Preparation and Properties of Piezoelectric Lead Zirconate Titanate Thin Films for Microsensors and Microactuators by Sol-gel Processing". Journal of the Ceramic Society Japan 104 (1996) 159-163
48. J.F. Shepard, F. Chu, I. Kanno, and S. Trolier-McKinstry, "Characterization and Aging Response of the d31 Piezoelectric Coefficient of Lead Zirconate Titanate Thin Films". Journal of Applied Physics 85 (1999) 6711-6716
49. L. Lian, and N.R. Sottos, "Effects of Thickness on the Piezoelectric and Dielectric Properties of Lead Zirconate Titanate Thin Films". Journal of Applied Physics 87 (2000) 3941-3949
50. H. Kueppers, T. Leuerer, U. Schnakenberg, W. Mokwa, M. Hoffmann, T. Schneller, U. Boettger, and R. Waser, "PZT Thin Films for Piezoelectric Microactuator Applications". Sensors and Actuators A 97-98 (2002) 680-684
51. K.Sumi, H. Qiu, H. Kamei, S. Moriya, M. Murai, M. Shimada, T. Nishiwaki, K. Takei, M. Hashimoto. Thin Solid Films 349 (1999) 270-275

52. G-T Park, J-J Choi, J. Ryu, H. Fan, and H-E Kim. Measurement of Piezoelectric Coefficients of Lead Zirconate Titanate Thin Films by Strain-Monitoring Pneumatic Loading Method. Applied Physics Letters Vol. 80, Number 24, 17 June 2002
53. X. Du, U. Belegundu, and K. Uchino. Crystal orientation dependence of piezoelectric properties in lead zirconate titanate: theoretical expectation for thin films. Jpn J. Appl. Phys. Vol. 36 (1997) pp. 5580-5587.
54. J.L. Devore, Probability and Statistics For Engineers and the Sciences, Sixth Edition. Brooks/Cole—Thomson Learning, Belmont, CA, (2004)
55. MINITAB Release 14. Copyright ©2004 Minitab Inc.
56. Lee M. R. Eakins, Development and Characterization of Materials in MEMS Power Generation. Masters Thesis, Washington State University
57. J. Chen, K.R. Udayakumar, K.G. Brooks, and L.E. Cross, "Rapid Thermal Annealing of Sol-Gel Derived Lead Zirconate Titanate Thin Films". Journal of Applied Physics 71 (1992) 4465-4469
58. K. Franke, H. Huelz, and M. Weihnacht, "Stress-induced Depolarization in PZT Thin Films, Measured by Means of Electric Force Microscopy". Surface Science 416 (1998) 59-67
59. A.L. Kholkin, S.O. Lakovlev, and J.L. Baptista, "Direct Effect of Illumination on Ferroelectric Properties of Lead Zirconate Titanate Thin Films". Applied Physics Letters 79 (2001) 2055-2057
60. B. Xu, Y. Ye, L.E. Cross, J.J. Bernstein, and R. Miller, "Dielectric Hysteresis From Transverse Electric Fields in Lead Zirconate Titanate Thin Films". Applied Physics Letters 74 (1999) 3549-3551
61. L.M.R. Eakins, B.W. Olson, C.D. Richards, R.F. Richards, and D.F. Bahr, "Microstructural Characterization and Mechanical Reliability of Interfaces in Piezoelectric Based Microelectromechanical Systems". Thin Solid Films 441 (2003) 180-186
62. F. Xu, F. Chu, and S. Trolier-McKinstry, "Longitudinal Piezoelectric Coefficient Measurement for Bulk Ceramics and Thin Films Using Pneumatic Pressure Rig". Journal of Applied Physics 86 (1999) 588-594
63. W. Ren, H. Zhou, X. Wu, L. Zhang, and X. Yao, "Measurement of Piezoelectric Coefficients of Lead Zirconate Titanate Thin Films by the Normal Load Method Using a Compsite Tip". Materials Letters 31 (1997) 185-188
64. APC International, Ltd. http://www.americanpiezo.com/materials/apc_properties.html